Measuring Individual Tree Water-use in Mature Native Species in the Pacific Northwest to Determine their Benefits for Stormwater Management

Phase 2 Final Report

By

Steven Quick[1], Dylan Fischer[1], Anand Jayakaran[2], Abby Barnes[3]

[1]Evergreen State College

[2]Washington State University

[3]Washington Dept. of Natural Resources

Prepared for

Water Quality Program at
Washington State Department of Ecology

On behalf of the **Stormwater Work Group**

February 2025, Publication 25-10-010

Stormwater Action Monitoring

Publication Information

This document was prepared for Ecology and the Stormwater Work Group as part of the Stormwater Action Monitoring Program. To learn more about the Stormwater Work Group or the Stormwater Action Monitoring collective, visit the websites listed in the related information section below.

This document is available on the Department of Ecology's website at:
https://apps.ecology.wa.gov/publications/summarypages/2510010.html

Related Information

- Stormwater Action Monitoring projects aim to improve stormwater management. Learn about current and past studies at the SAM website[1].
- The Stormwater Work Group (SWG) oversees the SAM Program. Visit the SWG website.[2] to learn more.

Contact Information

Water Quality Program
P.O. Box 47600
Olympia, WA 98504-7600
Phone: 360-407-6600

Website: www.ecology.wa.gov/SAM

ADA Accessibility

[1] www.ecology.wa.gov/sam

[2] https://ecology.wa.gov/about-us/accountability-transparency/partnerships-committees/stormwater-work-group

Table of Contents

List of Figures and Tables

Figures

Tables

Executive Summary

Urban trees in parks, natural areas, street-side and private lands can provide excellent opportunities to mitigate the effects of stormwater runoff in Puget Sound. While the runoff mitigation potential of forests or large tree stands is well known, there is still the need to quantify stormwater mitigation values associated with individual trees. This study was designed to continue and expand the SAM study's first Phase, which evaluated stormwater mitigation potential of individual local trees.

The Phase I tree study successfully developed a hydrologic dataset showing how mature native trees capture rainfall and mitigate stormwater. Phase I focused on mature trees in a forest setting. Interception patterns depended on tree canopy type and storm intensity, which likely scaled with canopy cover. Transpiration has two primary components: the speed of sap flux (movement of water up the tree stem; (hereafter, V) and the area over which water movement occurs within the tree stem (hereafter, SA). Both V and SA have been shown to vary among tree sizes and tree species. Street trees are likely to vary in size and species composition compared to native mature trees. Accordingly, Phase II (this report) focused on determining the effects of tree size on the speed of transpiration and scaling estimates of whole tree transpiration (hereafter, F) from mature trees to street trees in a model system and using new sap flow measurement technology. Younger and smaller trees are more common in an urban context, especially near impervious surfaces, and require new measurement techniques. This technique was additionally tested against existing technology to ensure accuracy. Phase II of this study had four primary goals: 1) Quantify variation in V associated with tree size in two dominant mature species measured with traditional sap flow technology 2) Validate the usefulness of a new mobile sap flux measurement technology by comparing patterns in sap flux among trees instrumented with both traditional measurement technology and a new mobile unit technology; 3) once validated, measure example street trees in a typical street tree environment, and 4) place all measurements in the context of precipitation inputs, interception, and local weather variation.

We found that 1) V did not vary by tree size in either model deciduous species (bigleaf maple, Acer macrophyllum) or a model coniferous tree (Douglas-fir, Pseudotsuga menziesii); 2) patterns in V for trees instrumented with traditional and new mobile technology were identical – supporting the use of the new technology as a reliable approach for estimating street tree water-use; 3) whole tree water use varied significantly by species in both amount and timing. As in Phase I, the deciduous tree, bigleaf maple, transpired much less water in shoulder seasons (Spring and fall), while Douglas-fir may reduce water transpiration in summer. Three different street tree species (one conifer and two distinct hardwood species) show subtle differences in growing season (Spring-Fall) transpiration patterns and amounts. Finally, 4) in the context of whole-year water budgets, we estimate that the sum of mitigation (transpiration and interception) was ~ 71 cm of water annually for the conifer tree species we studied (Douglas-fir). In comparison, a deciduous tree species (bigleaf maple) mitigated 89 to 103 cm of water from canopies. Compared to rainfall in an average year at our site (approximately 130 cm), street tree canopies cumulatively could result in a 42-66% reduction in precipitation in street tree soils and impervious surfaces.

Introduction

This report summarizes the results of the Phase II portion of a multiyear project evaluating tree water use and interception patterns in forests and semi-urban environments.

Study Need

Urban trees in parks, natural areas, street-side and private lands combined with other green stormwater control elements provide excellent opportunities to mitigate the effects of stormwater runoff in Puget Sound, the Lower Columbia River, and other important waterways in western Washington. While the runoff mitigation potential of forest or large tree stands is well known, there is still the need to quantify stormwater mitigation values associated with individual trees. In Phase I of this project, we demonstrated differences in transpiration and interception amounts and timing for two common coniferous (Douglas-fir, *Pseudotsuga menziesii*, and western redcedar, *Thuja Plicata*) and two common deciduous species (bigleaf maple, *Acer marcophyllum*, and red alder, *Alnus rubra*) in urban-adjacent south Puget Sound forest locations.

The overall goal of this Phase II project was to 1) validate that findings from Phase I apply across a range of tree sizes and 2) continue to quantify and refine stormwater mitigation values of young and isolated conifer and deciduous trees in streetside and parking lot locations in western Washington using a new and novel mobile transpiration device. Two sap flux systems from the original Phase I study were deployed at the previous study locations on The Evergreen State College (TESC) campus. These two sap flux setups ensured that Phase I and Phase II of the studies related to continuously logging sensors that helped maintain the continuity of the data record and the associated variability of sap flux data. Ten Douglas-fir trees and ten bigleaf maple trees were monitored as part of this work. This study phase measured transpiration rates and canopy interception across various tree sizes.

Phase II was designed to target more visible and younger trees, requiring better security for equipment and a power supply. However, this created a challenge for sap flux technology, which required proximity to a power source and the installation of large semi-permanent instrumentation. Washington State University (WSU) and TESC developed a smaller, discrete, cheaper mobile data logger with its power supply to account for this challenge. These mobile data loggers were connected to the identical thermal dissipation probes (TDP) in Phase 1. They were deployed for 24-48 hours on 10-20 trees per measurement event for at least 12 measurement events per year. This ensured that the devices were not left out in the open for extended periods, minimizing the likelihood of vandalism and theft. Measurement events occurred across multiple locations (new locations/trees for each event), maximizing the inference for street tree water use across the region. Accordingly, our sample design comprised two sets of sample trees. Trees from Phase I continued to be measured - designated as “Phase I Confirmatory” (PIC) - and those new and smaller trees measured in this Phase were designated as “Phase II Experimental” (PIIE). First, we selected “Phase I – Confirmatory” trees across a range of diameters at the location of the Phase I sap flux installation. The range allowed us to quantify any potential changes (or lack of change) among varied trees, enhancing our confidence in extrapolating our findings to various small and large trees in developed areas.

Older and larger (<12 inches DBH; diameter at 4.5 feet above the ground) trees were also less sensitive to damage and thus presented better opportunities for repeatedly installing the newer Phase 2II sensors without damaging the permanently instrumented tree (e.g., repeated drilling in small trees can result in long-term damage and affect our estimates of transpiration). The instrumented trees at the Phase I location on the Evergreen State College campus allowed a direct comparison of measurements taken using the standard sap flux setup and the newer Phase II probes. Thus, our PIC tree design had three purposes: 1) establish the nature of the relationship between tree size and sap flux rates, 2) provide consistent measurements in trees that are more resistant to damage from repeated probe installation, and 3) provide the opportunity to directly compare transpiration estimates from static and mobile sap flux setups – providing a quality check on the newer mobile unit approach.

Specific project objectives for the PIC were:

- Establish baseline relationships between tree size and sap flux for two of the most common trees in our region: a coniferous evergreen tree (Douglas-fir) and a deciduous angiosperm tree (bigleaf maple). These baseline relationships provided better information for applying Phase I results to trees of variable size in the region.
- Use data representing a continuation of a multiyear dataset on annual transpiration rates to ensure quality control for a newer mobile sap flux measurement approach.

Specific project objectives for the PIIE were:

- Extend sap flux sampling to urban trees in developed areas using a mobile sap flux technology approach. Provide robust estimates for urban tree transpiration based on empirical estimates.
- Estimate annual canopy interception rates for the same trees based on Phase I results and opportunistic sampling at trees in urban or developed locations (trees planted in medians, sidewalks, or islands near paved locations.

Methods

Study Design

The Phase II study involved instrumenting 40 trees in the Olympia area to determine the transpiration rates of two species of native trees, comprising one coniferous and one deciduous tree species, and two additional species of hardwood street trees (red maple, *Acer rubrum*, and honey locust, *Gleditsia triacanthos*). Of these 40 trees, all were instrumented to measure sap flux and 16 for canopy interception. Two weather stations were installed to measure microclimatic variability and soil moisture was collected weekly at each tree.

Douglas-fir and bigleaf maple trees were selected for the PIC trees due to their conventional roles and ubiquity in the PNW region. These trees are frequently found in residential neighborhoods and vacant sites within community growth management areas. Tree species selected for the PIIE trees depended on their availability in developed parking lots, but also represented common street trees in new developments.

Study Site

The study locations in the south Puget Sound region near Olympia, WA, were at The Evergreen State College (forest site and parking lot site; Figure 1). The sites are 0.85 miles apart. These locations experience slightly different micro-climates despite their proximity due to unique land use features such as forested green spaces and impervious surfaces. Sites represented locations that would typically face development in a rural-urban interface, the interface that is seeing the greatest land use changes in western Washington.

Both locations were identified as forested, but one represents a more moderate development scenario. Based on historic aerial imagery and local knowledge, the forest site was last subject to timber harvesting in the 1950s and 60s, making many mature trees at least 50 years old. For logistical consistency with Phase I of the study, the forested site was divided into two "plots" (Plots 1 and 2) which reflect the instrumentation for the sites more than a physical barrier (the plots are directly adjacent to each other but are instrumented separately). The parking lot site (also referred to as Plot 3) was cleared for a parking lot in the late 1960s. Critically, both sites offered power, security, and full-time equipment access. While various forest habitat conditions were present across sites, all locations were free from invasive plant species prevalent in western Washington that may impact tree health, such as English ivy, scotch-broom, and Japanese knotweed. The second location (the parking lot site) is an active parking lot with planted trees in tree islands.

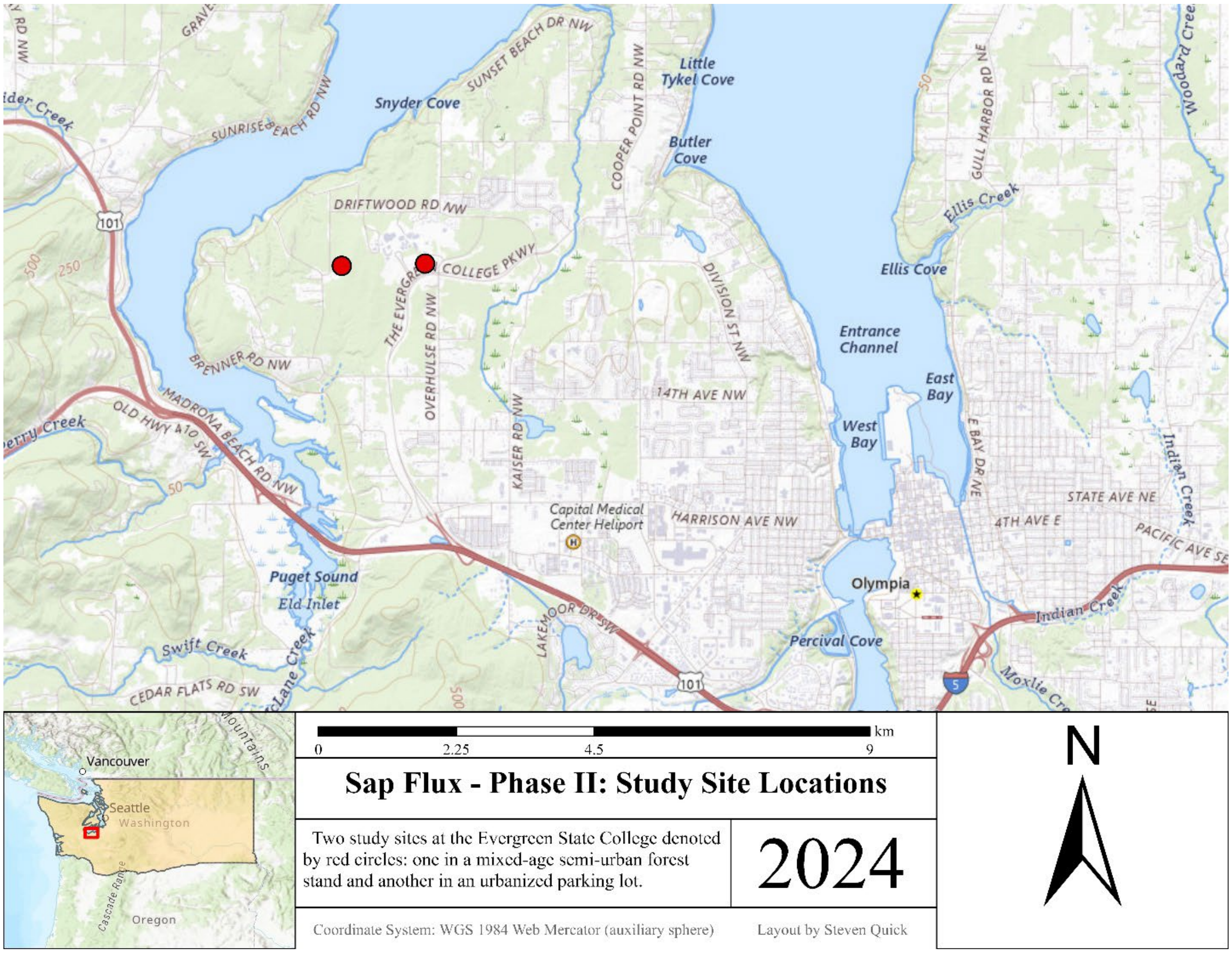

Figure 1. Map of the south Puget Sound region of Washington State showing the two study locations near the Evergreen State College in Olympia. Red-filled circles denote study sites. Plots 1 and 2 are located adjacently in the westernmost red dot. Plot 3 is the east dot.

Tree Selection

Of the many differences between candidate tree species, it was decided that the difference between coniferous and deciduous species would have the greatest impact on the study from an eco-hydrological perspective. Therefore, one of each type was chosen based on overall prominence in the region, availability at each of the study sites, and greatest importance to water budgets described in Phase I. Douglas-fir is an evergreen conifer, while bigleaf maple is a deciduous broadleaf species. The trees chosen for the PIC portion of this work comprised 10 bigleaf maple and 10 Douglas-Fir (Table 1, Figure 2). Due to interest in the effect of tree size on sap flux, trees were also selected to represent a size gradient at the forested site, while trees at the parking lot site (plot 3) were all less than 30 cm (about 12 in) DBH. For the PIIE portion of the study, we chose 10 additional Douglas-fir trees adjacent to paved surfaces or parking lots on the Evergreen State College Campus (Table 2, Figure 3-4).

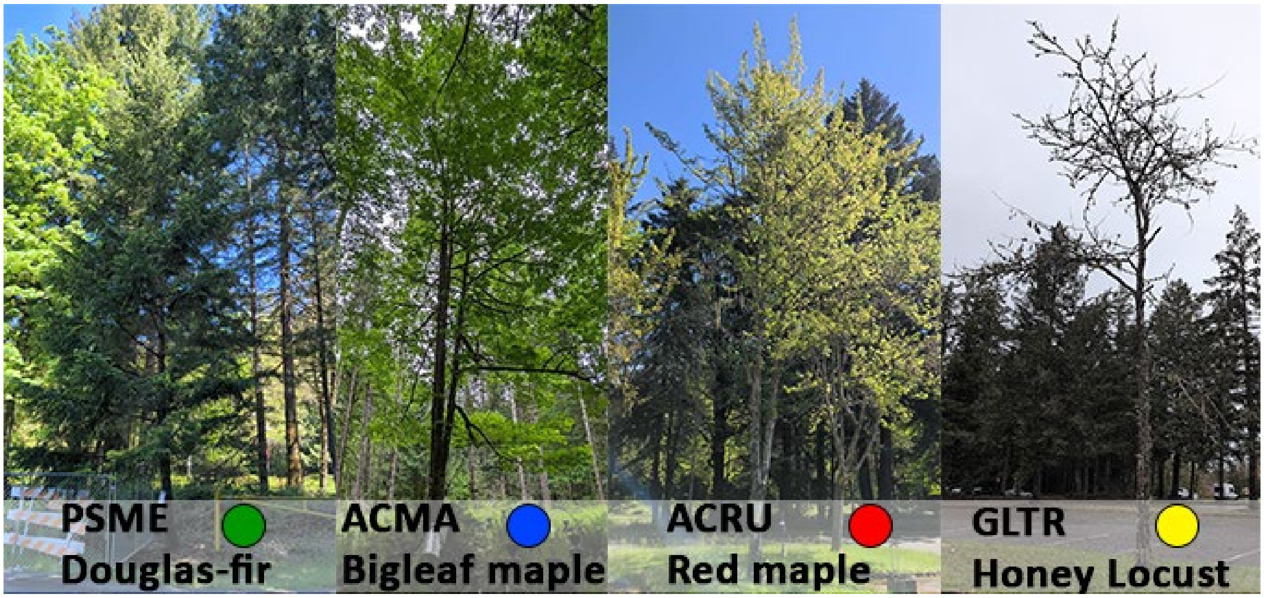

Figure 2. Winter/spring pictures of the two four natural forest tree species chosen for this study. Colored circles match legend.

Table 1: Selection of trees included in the study by plot and species where each tree was measured for sap flux and throughfall.

Location	**Douglas-Fir** ***Pseudotsuga menziesii***	**Bigleaf Maple** ***Acer macrophyllum***	**Red Maple** ***Acer rubrum***	**Honey Locust** ***Gleditsia triacanthos***
Forest Plot 1	5(2)	5(1)		
Forest Plot 2	5(1)	5(2)		
Parking Lot Plot 3	10(5)		7(5)	3(0)
Total	20(8)	10(3)	7(5)	3(0)

Notes: Parentheses "()" indicate the number of trees with rain gauges measuring throughfall precipitation.

Figure 3. Representative trees in the PIIE study. Photos taken in Spring 2024.

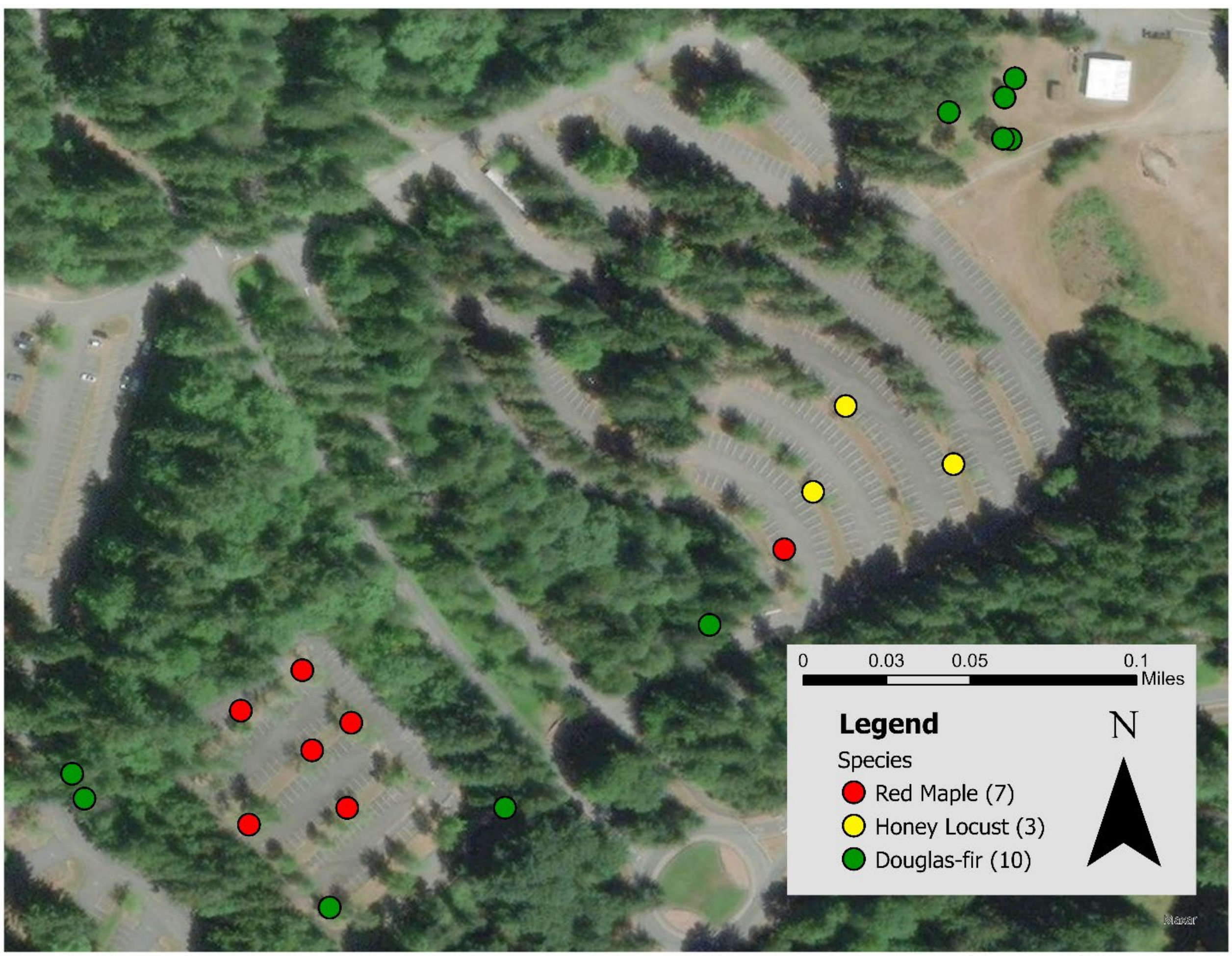

Figure 4. Aerial image of Parking Lot (Plot 3) street tree locations where trees were located for this study.

Environmental Data

General environmental data were collected to identify site-specific climate trends and develop final tree water-use calculations for interception and transpiration (Table 2). Precipitation data were of greatest importance in calculating water use in relation to the total rainfall for a period of interest. These rain gauges were attached to larger weather stations that collected other measurements to assess ambient conditions. Other environmental data were collected with separate equipment deployments for plot-specific soil moisture.

Some of this data was used to explain direct measurements of water use. For example, it was expected that transpiration rates should be impacted by several variables, including a) the intensity of photosynthetically active radiation (PAR), b) the availability of soil water in the root zone (soil moisture), and c) the potential direct evaporation of water from a leaf's surface as dictated by the vapor-pressure deficit (VPD). VPD is calculated from measurements of air temperature and relative humidity using the standard Tetens equation to solve for saturated vapor pressure:

$$e_s(millibars) = e^{\left(\frac{(17.269*T)}{(237.3+T)}\right)} \times 6.1078$$

where e_s is saturated vapor pressure in millibars, T is temperature in °C, and vapor pressure deficit is calculated as

$$VPD = e_s - \frac{Rh \times e_s}{100}$$

Where Rh is relative humidity.

Table 2: Summary of all equipment deployments with the number of sensors and installation dates for each site. Environmental data equipment deployments not associated with direct individual tree water-use measurements are shown in bold font.

	Window of Deployment		
	Forest (Plots 1 and 2)	Parking Lot (Plot 3)	# of Sensors
Sap Flux	June 2019-August 2024	April 2023-August 2024	20 per site[a]
Throughfall	May 2023 – August 2024	May 2023 – August 2024	34 total[b]
Weather Station	**April 2023 – August 2024**	**May 2023 – August 2024**	**8 per site[c]**
Soil Moisture	May 2023 – August 2024	May 2023 – August 2024	1 per week[d]

Notes: a: 20 trees per site, 1 sensor per tree. b: Two sets of rain gauges arranged along two transects at mid-canopy and dripline for 6 trees at the Forest site. One rain gauge was placed mid-canopy for 10 trees at the Parking Lot. c: 8 sensors collected 11 variables at each site. d: collected instantaneously once per week

Weather Stations and Data Loggers

Weather stations were set up in fields near the forest site (Plots 1 and 2) and Parking Lot (Plot 3) at least 300 feet from large obstructing objects (buildings, etc.) and stabilized with guy wires and grounding anchors (Figure 4). A total of 9 parameters were recorded by each weather station (Table 3). Additional rain gauges not associated with the established weather stations were deployed under tree canopies to measure throughfall. All weather stations and rain gauge sensors recorded measurements every minute. Data were uploaded to the Hobolink cloud using a RX-3000 data logger every hour. Weekly data summaries were downloaded and post-processed to average measurements every hour, and then daily, for agreement with tree sap flow measurements (see below).

Figure 5 Weather station placed in a field north of Parking Lot site.

Table 3: List of weather station parameters measured. Units are in parentheses.

Weather Station Parameter	Range of Values
Air Temperature (°C)	-7.6 to 37.5
Dew Point (°C)	-10.5 to 24.5
Leaf Wetness (%)	0 to 100
PAR (µE)	1 to 2377
Pressure (millibars)	660 to 1031.9
Rain (mm)	0 to 13.7
RH (%)	0 to 100
Solar Radiation (W/m2)	1 to 1204.7
Wind Direction (°)	0 to 358

Soil Moisture Measurements

Plot-level soil moisture was measured directly each week at each tree using a Hydrosense II (Campbell Scientific, Inc.). This device measures volumetric water content (VWC) using the Time Domain Reflectometry (TDR) measurement principle. Compared to capacitance sensors used in Phase I, this TDR sensor is more resistant than autonomous equipment to environmental factors. This is a portable instrument, so measurements had to be manually planned and executed by field staff for each measurement day.

Interception Estimates

Throughfall

A total of 16 trees were instrumented for the measurement of canopy throughfall: 6 with a two-by-two array of rain gauges located at mid-canopy and dripline and 10 with a single rain gauge located at mid-canopy (Table 1;Figures 6-7). Throughfall was determined in situ by comparing closed-canopy measurements to open-canopy weather stations. Throughfall can be expressed as a depth (cm) or as a fraction of the rainfall measured in an open canopy:

$$Throughfall_i(\%) = \frac{\sum Precipitation_{cc_i}}{\sum Precipitation_{oc_i}} * 100$$

Where:

- *Precipitation*$_{cci}$ is the total rainfall (cm) measured under the tree canopy or closed canopy (cc),
- *Precipitation*$_{oci}$ is the total rainfall (cm) measured under the open canopy (oc),
- And *i* indicates the period of interest

For more details on throughfall methods used, please see Appendix A from the Phase I Final Report.

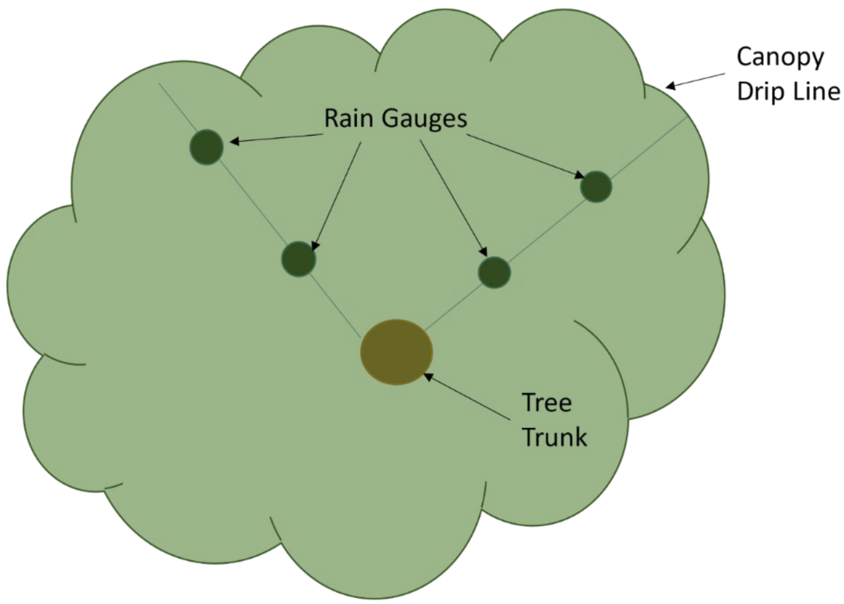

Figure 6. Profile (top) view of rain gauges used to measure canopy throughfall.

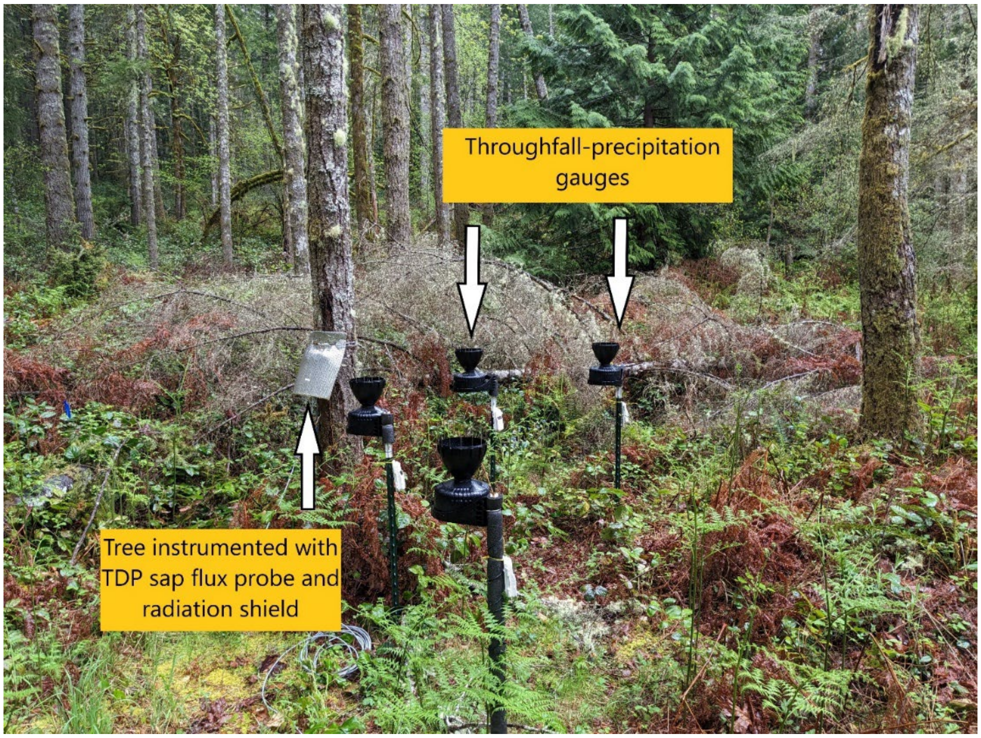

Figure 7. Arrangement of rain gauges at Evergreen forest site.

Transpiration by Sap Flux

Transpiration, a critical component of individual tree water use, is typically calculated using direct sap flux measurements. The sap flux thermal dissipation probe (TDP) technique involves measuring the temperature difference between heated top and unheated bottom probes inserted into the tree's xylem. As sap moves upwards during transpiration, the heated probe is cooled, and the temperature difference between probes is diminished (Granier 1994).

Using the Granier equation (see Jayakaran et al. 2022, Steppe et al. 2010, Oishi et al. 2016), sap flux velocity or density (hereafter, V) is calculated from the TDP probe data as the flux of water per unit area of sapwood with units: g of H20/ cm2 of sapwood/ second. The calculation is based on determining daily maximum heat differences between paired heated and unheated probes in the tree. We used the widely adopted software package Baseliner for fixed-station trees to process V values for all trees (Oishi et al. 2016). Data were filtered according to Baseliner defaults for reasonable temperature differences between probes (typically between 2 °C and 20 °C, with a typical day-night difference of less than 5 °C), and data were only included for days with continuous datasets over 24-hour periods without breaks in the data due to power outages or voltage spikes. For mobile-unit sap flux data (see below), all data were processed with Dynamax's template Excel sheet for processing sap flux data (https://dynamax.com/images/uploads/papers/TDP_SapVelAnlyser.xlsx , last accessed 10/31/2024).

For questions related to comparing patterns in V with tree size and patterns in water use between probe types, we used comparisons of V since they are empirically independent of differences in tree architecture, such as in the sapwood area. Values were summed by day for analyses and then averaged through time, resulting in estimates of V in units of g H_2O cm^{-2} sapwood day^{-1}.

The daily whole tree transpiration (F; L of H_2O day^{-1}) is calculated by multiplying the speed of sap flux through the tree bole (V) with the sapwood area over which water moves. Accordingly, daily V (cm^3 H_20 cm^{-2} sapwood area day^{-1}) is transformed to daily transpiration using the following equation:

$$F(L) = (V_b * \ Sapwood\ Area_b) * 0.001$$

Sapwood $Area_b$ is the sapwood area (cm^2), and V_b is V for each tree b. A multiplier of 0.001 is used to convert cm^3 to L.

Previous studies have also accounted for variation in V with depth in the sapwood (radial variation). Still, our studies in Phase 1 confirmed a lack of significant, predictable radial variation in our measurements. Accordingly, as shown above, all our measurements used an average estimate of V per tree, multiplied by the sapwood area of said tree.

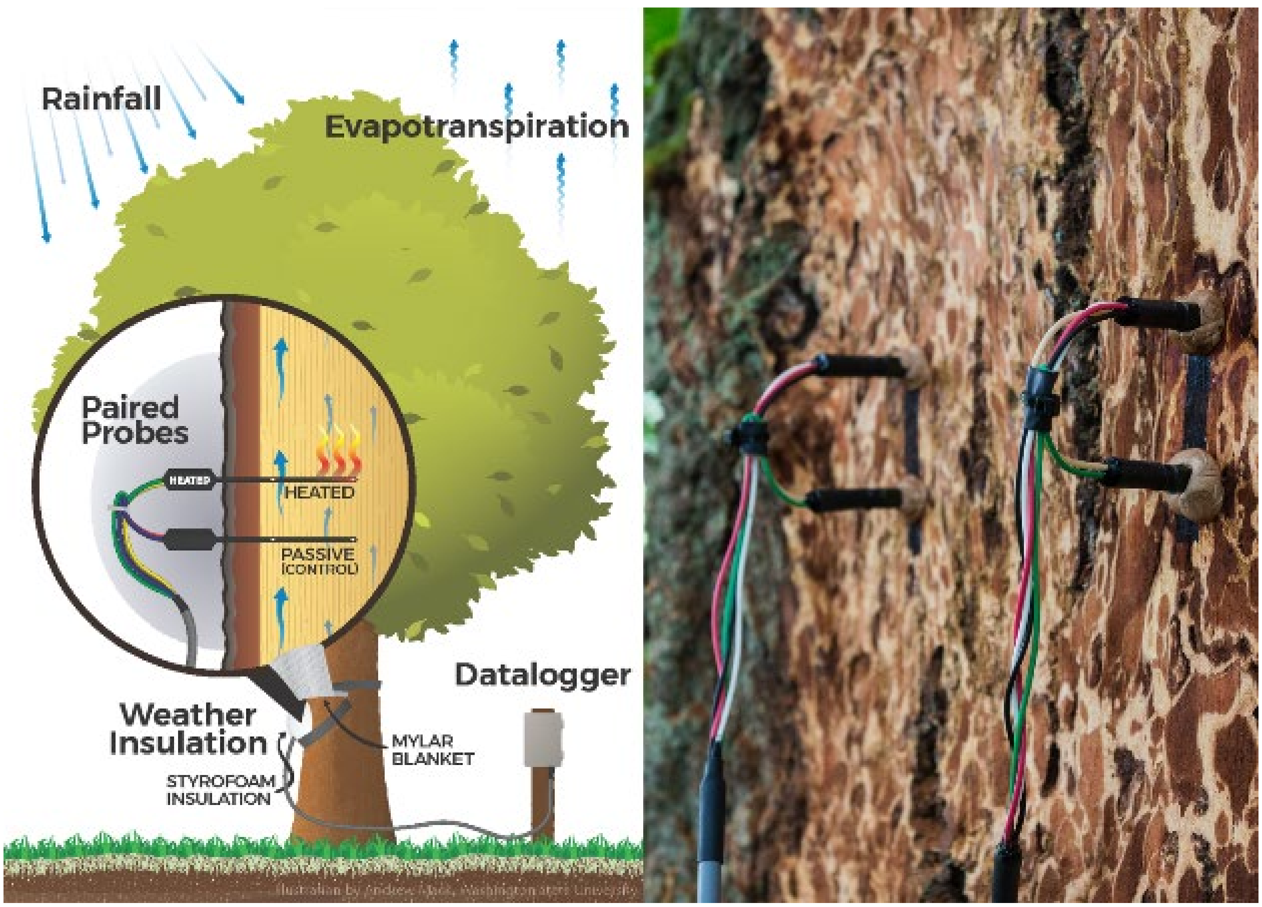

Figure 8. Diagram illustrating the thermal dissipation probe (TDP) method for measuring sap flux (left) in addition to two sets of probes inserted into a Douglas-fir (TDP-50 [left]; TDP-100 [right]) where excess bark has been removed and insulation has yet to be installed.

Fixed-Station Sap Flux Units (Plots 1 and 2)

We selected equal numbers of trees among available Douglas-fir (PSME) and bigleaf maple (ACMA) within 170 ft of each of two central fixed station data logger sites (Plots 1 and 2; Figures 9 and 10). Plot 2 was slightly uphill from Plot 1 (Figure 10), and several larger trees were found in site 1. Such design limitations were inherent due to the fixed-location nature of the standard sap flux station design. Accordingly, there may be autocorrelation in sap flux patterns in trees by station, and such bias should be considered when using these data.

Finally, one permanent TDR probe for soil moisture was also installed at Plot 2 to provide a baseline measurement of soil moisture during the study (Figure 11).

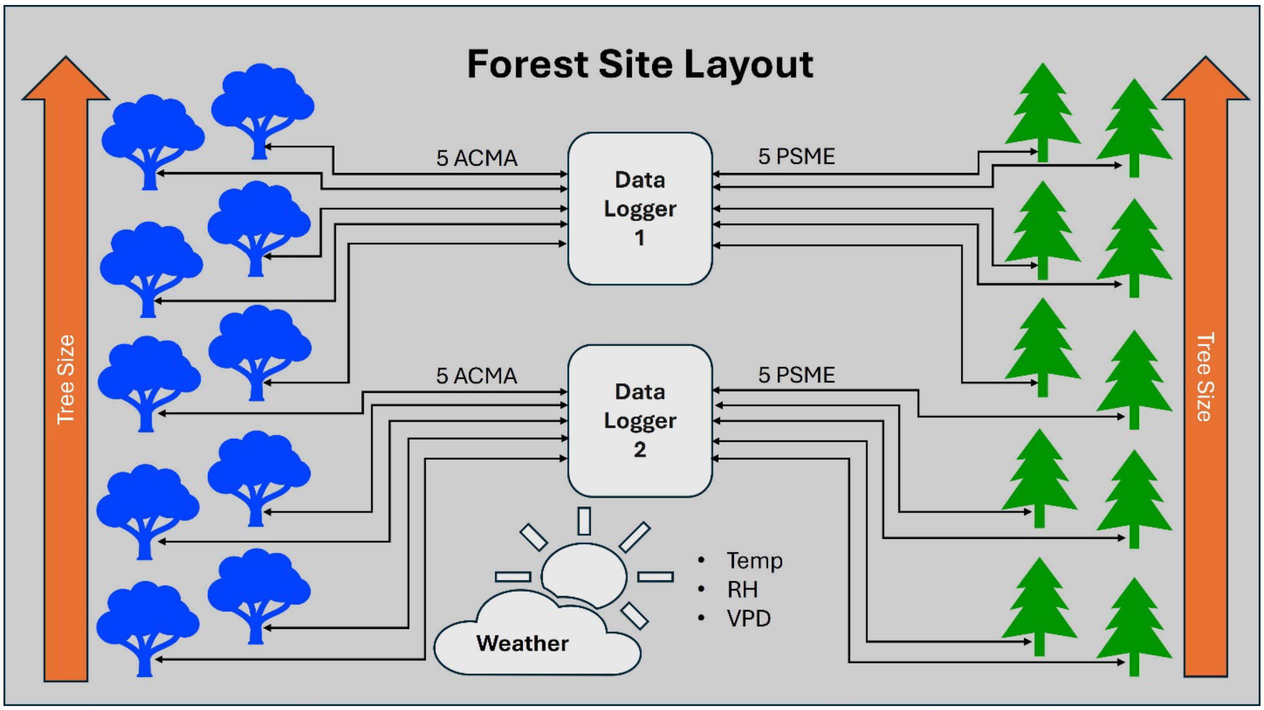

Figure 9. General schematic for fixed- station sampling of forest trees. Trees were selected to represent a gradient in tree sizes. While the diagram depicts maple ACMA (blue) in one direction and PSME (green) in another, the trees were generally interspersed (PSME adjacent to ACMA) at each site, and they are only separated here for schematic clarity.

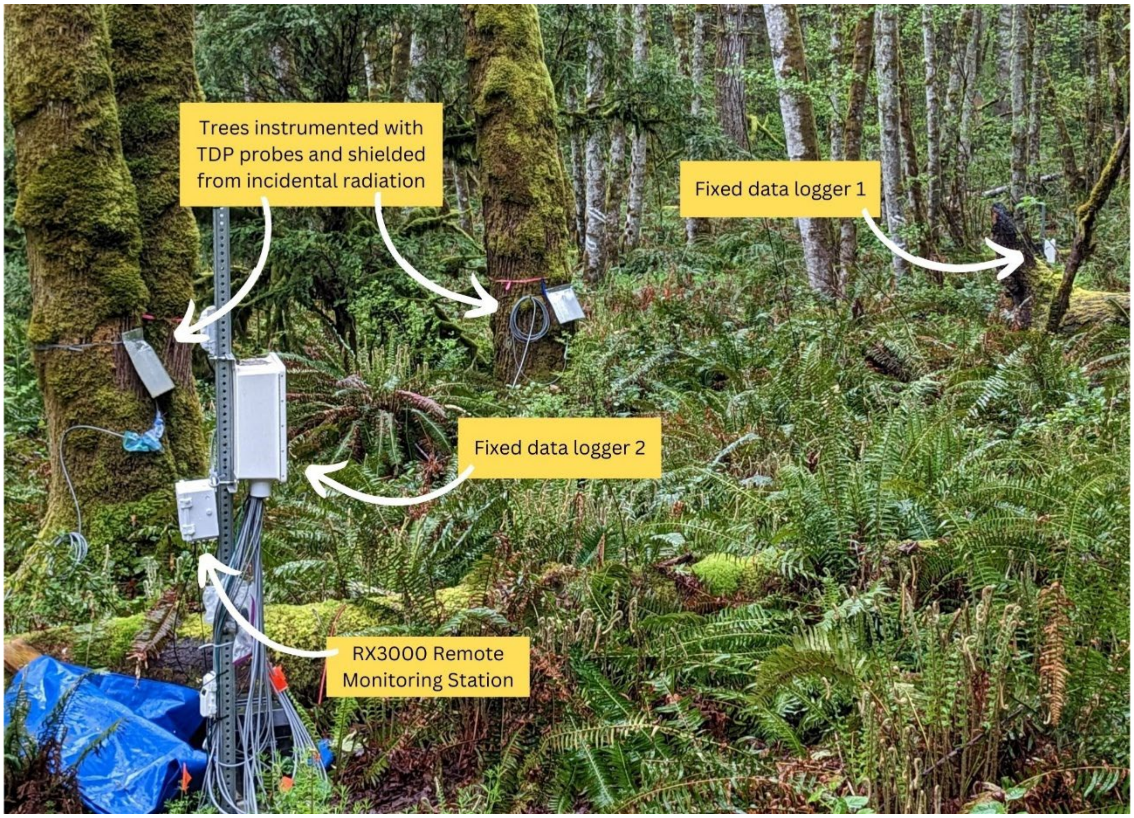

Figure 10. Trees instrumented with sap flux monitoring probes are connected to a stationary datalogger installed on Plots 1 and 2. A RX3000 remote monitoring system is installed at Plot 2 and connected wirelessly to 24 throughfall-precipitation gauges.

Figure 11. Soil moisture at Plot 2 station is continuously monitored using time domain reflectometry probes (Campbell Scientific), sampling every minute and reporting 15-minute averages.

Mobile Sap Flux units

While traditional sap flow methods have a restricted footprint, we used a modified mobile sap flux measurement design based on Arduino miniaturized computers and small 12-V batteries in water-proof mobile cases. The design uses the identical sap flux probes described above (made by Dynamax Inc. Houston, TX). Still, instead of a fixed-station Campbell datalogger connected to continuous AC power, the mobile system uses a hand-built voltage regulation system and miniature Arduino computers (programmed as dataloggers) connected to a mobile DC power source. The devices are then transportable to individual trees instrumented with sap flow probes (Figure 12-13).

To test the utility of these devices, we first conducted detailed in-house QA/QC for building and deploying the systems (see Appendix A: SOP for Mobile Units). Next, units were installed in trees and monitored using traditional fixed-station dataloggers and power methods (see above).

A comparison of patterns in V using the two setups allowed verification that the mobile units were measuring similar patterns.

Finally, mobile units were deployed during 2023-2024 on pre-determined study trees in highly visible semi-urban parking lot locations (Plot 3; Table 1-2, Figure 4, 12-13). Initial testing indicated optimal deployment was for 3-4 days to measure trees using days 3-4 of each cycle. In 2023, initial deployments began at 4-days per unit, with two days of measurement per mobile device. Subsequent testing determined battery health declined in units deployed for 4 days, and 3-day deployments were a more realistic long-term strategy for maintaining device battery health. Hence, deployments in 2024 were for 3-days, producing a single day of usable data per deployment. Trees sampling strategy was stratified to yield roughly one day of measurement per month for each tree in the study throughout the growing season.

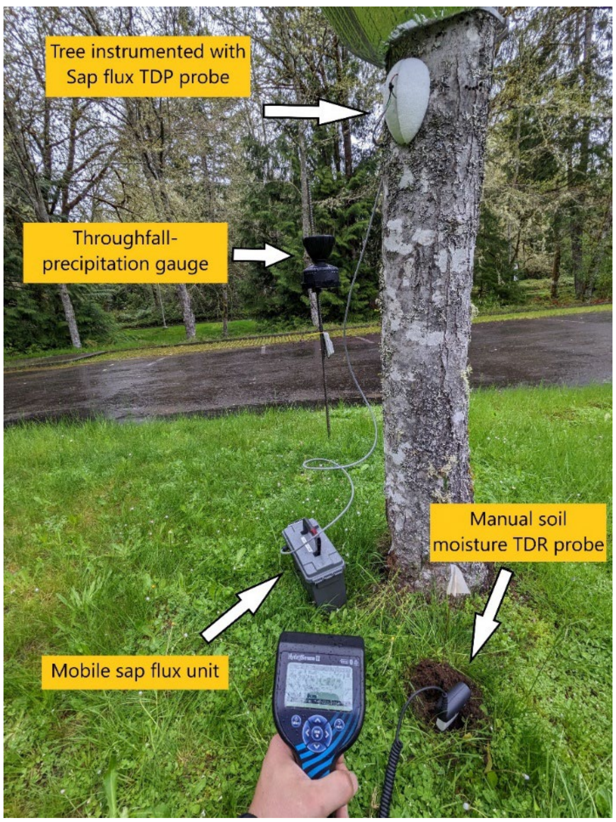

Figure 12. Mobile sap flux units are deployed weekly at site 3, and manual soil moisture measurements are collected at each tree on all three sites. One rain gauge is installed beneath each of 10 tree canopies at one-half of the radial canopy distance.

Figure 13. Details on mobile probes. Washington State University (WSU) and TESC developed and deployed a mobile data logger (smaller and cheaper than the traditional approach) at twenty street tree locations in 2023 and 2024. These mobile data loggers are deployed for 2-3 days at a time, and the 2nd or third day is used for sap flux data (allowing the first day for equilibration of the heated probe to the tree).

Canopy Area Field Methods

The trees were assumed to be geometric paraboloids to estimate the canopy's projected surface area ($Area_{can}$) where

$$Area_{can} = \pi \times \left((CrownDiameter1)/2 \times (CrownDiameter2)/2\right)$$

This assumption enabled the estimation of canopy area from the crown diameters and at the crown base taken along north-south (CrownDiameter1) and east-west (CrownDiameter2) transects.

Individual Tree Water Budgets

Total Tree Water Budget Calculations

The total tree water budget can be considered the fraction of rainfall that a tree assimilates through transpiration and interception. It can be expressed volumetrically (cm^3) or as a fraction (%) of the total rainfall falling on that tree's canopy area (cm^2) over a specific time. The tree water budget in volumetric terms can be defined by:

$$Tree\ Water\ Budget\ (cm^3) = Transpiration(cm^3) + Interception(cm^3)$$

This assimilated water, or the tree's water budget, is the stormwater volume avoided or removed from runoff conveyance systems. In volumetric terms, this runoff volume (cm3) is:

$$Runoff(cm^3) = [Precipitation * CanopyArea] - TreeWaterBudget$$

We define Interception (cm^3) as:

$$Interception\ (cm^3) = [Precipitation * CanopyArea] - (Throughfall)$$

Our previous work (Phase I) established that stemflow (intercepted water running down tree stems) was minimal, even in high-volume precipitation events. Accordingly, it is not accounted for here, and this should be considered when using these data. A comprehensive measure of a tree's water budget can be calculated as follows:

$$Tree\ Water\ Budget_n(cm^3) = \sum_{i=1}^{n}(Transpiration_i + [Precipitation_i * CanopyArea] - [Throughfall_i])$$

where n is the total number of days in a specific time period (season, year, etc.), and i represents a given day for a given tree.

To express the Tree Water Budget as a fraction of rainfall, the volumetric water budget (cm^3) was first normalized by canopy area (cm^2) using:

$$CanopyNormalizedTreeWaterBudget_n\ (cm) = \frac{Tree\ Water\ Budget_n}{Canopy\ Area}$$

The Tree Water Budget expressed as a fraction of the total precipitation (qualifying storm totals, units = cm) that occurred over the year was calculated by:

$$TreeWaterBudget_{year}(\%) = \frac{\sum_{i=1}^{n} CanopyNormalizedTreeWaterBudget_i}{Annual\ Precipitation\ Total} * 100$$

where n is the total number of days.

Results & Discussion

PIC: Relationship Between Tree Size And Sap Flow Dynamics

A primary goal of Phase II was to ensure results from Phase I were scalable across trees, which are variable by size. It was first important to determine the existence of a relationship between tree size and sap flux velocity (V).

Figure 14 shows sap flux data for 2023 measured at the fixed stations, where average daily V is grouped by species and three VPD classes (based on natural breaks in the data: low, 0.6-1.2 kPa, medium, 1.2-1.7 kPa, and high, 1.7+ kPa). Initial analyses from this year suggested that linear regression relationships between DBH and sap flux were highly dependent on VPD. All relationships were initially statistically significant ($P < 0.05$), but relationships were also generally weak (Mean $r^2 = 0.2\text{-}0.6$). When comparisons were limited to only coincident days for trees across all sizes, DBH was not a significant predictor of V for either native species (PSME and ACMA) (Figure 14). Limiting the data to coincident days is critical since tree water-use patterns can vary by day, and if probe failures were present on some days for only some trees, data from those days would not produce the same average results. In other words, probe failure can lead to uneven sampling across tree sizes in different days, which could introduce accidental biases. For example, if small trees were sampled early in the season, and large trees late in the season, we might conclude that small trees differed from large trees, but time-of-season would be a hidden factor. Sampling on coincident measurement days ensures all data comes from the same time periods for all trees. Taken together, these data suggest that while relationships can be found for DBH and V, especially in bigleaf maple during low VPD periods, on average V is independent of tree size in young mature trees for both bigleaf maple and Douglas-fir.

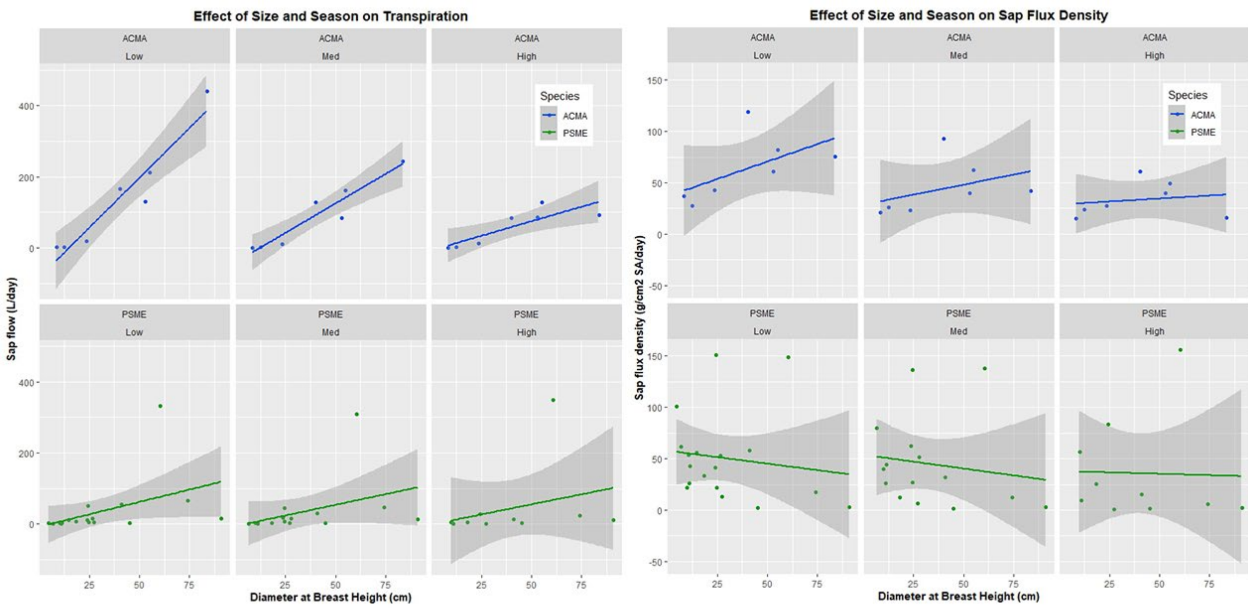

Figure 14. Transpiration (F) and Sap Flux Density (V) from 2023 and 2024 data versus tree size (DBH) separated by VPD class (based on natural breaks in the data: Low, 0.6-1.2 kPa, Medium, 1.2-1.7 kPa, and High, 1.7+ kPa).

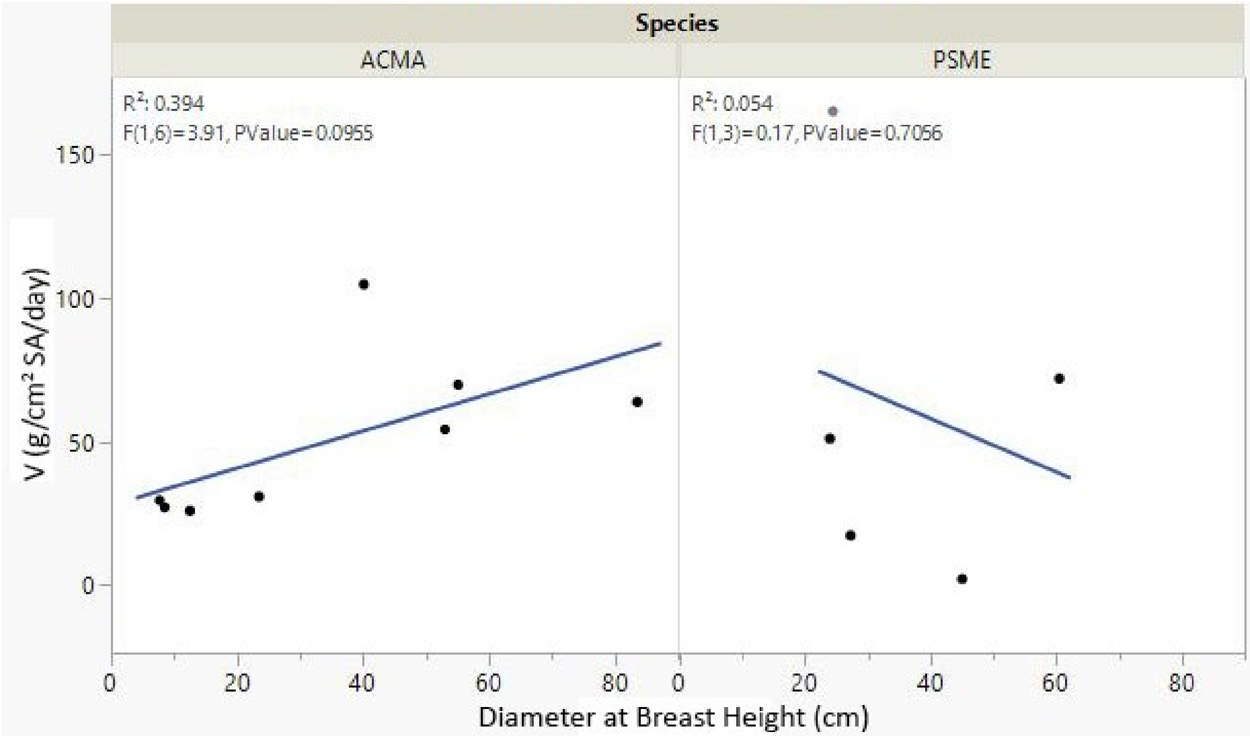

Figure 15. Average Sap Flux Density (V) by tree size. Values were averaged from coincident measurement days only (when data was available for all trees in the study during the growing season). Linear regression statistical results are shown in the upper left of each panel.

Accounting for differences in sapwood area allows calculation of total transpiration per day, which scales strongly with tree size, primarily because larger trees inherently have greater sapwood area. Values of F inherently increase with tree size (Figure 16).

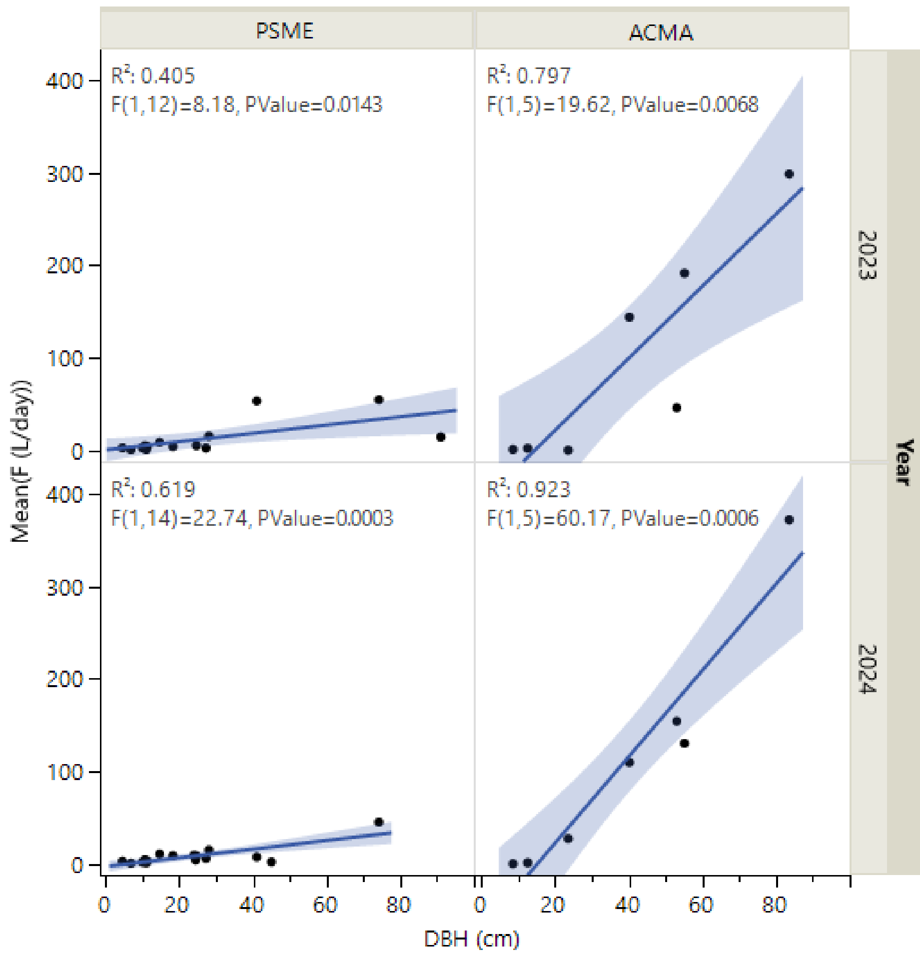

Figure 16. Total tree average daily transpiration during the growing season by tree size (DBH). Results of linear regression analyses are shown in each panel.

PIIE: Validation Of The Mobile Unit Approach

Using the mobile units and fixed-station approach, we evaluated coincident sap flux density measurements in the same trees in 2023. The graph below (Figure 17) shows patterns in V for two sets of probes installed in the same tree on the same day. The comparison validated the quality of estimates from the mobile approach. Comparisons showed reliable and realistic measurements from the mobile unit probes using this approach. In some cases, values differed due to differential contact of the probe with conductive sapwood tissue. Still, errors were not beyond what we expect in probe-to-probe comparisons using traditional sap flux methods.

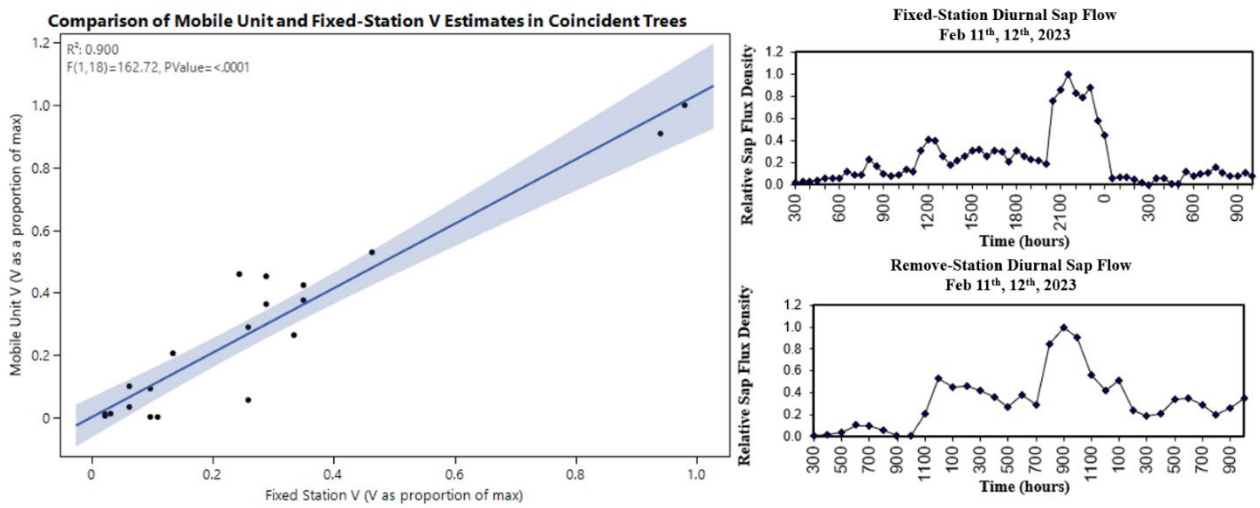

Figure 17. Comparison of relative values from a single tree instrumented with traditional fixed-station and new mobile unit sensors. Left: a direct comparison of relativized values from both methods generating a slope of approximately 1 and close alignment of data from each method (statistical results of a regression analysis are presented along with an R2 value indicating goodness of fit. The slope of the regression line was 1.01). Right Top: an example diurnal curve from a tree instrumented with fixed-station sap flux methodology February 11-12, 2023. Right bottom: example data from the same tree simultaneously instrumented with mobile unit probes.

PIIE: Transpiration And VPD Throughout The Year

Measurements of V across the four species showed that vapor pressure deficit (VPD) and soil moisture displayed patterns in determining sap flux that were similar to patterns observed in other studies (Figure 18). All species' transpiration, as calculated from V and sapwood area, was mildly, but not strongly, correlated with VPD. The results of polynomial regression predicting V from VPD demonstrated weak (r^2: GLTR = 0.4, ACRU = 0.2, PSME = 0.008, ACMA =0.047), but significant ($P < 0.05$) relationships. For Soil Moisture, relationships were similarly weak (r^2: GLTR= 0.12, ACRU = 0.03. PSME = 0.03, ACMA = 0.11; Figure 18).

A common analysis approach with VPD and Transpiration data, termed "boundary-line analysis", considers only the top 10% of sap flux data (here represented by V) within VPD (x-axis) bins. This approach has been employed in numerous sap flux studies examining tree physiological responses to environmental variables (e.g., Fischer et al. 2002). Such an approach clarifies the nature of the responses of V to VPD, and is shown in Figure 18, where all trees demonstrate a curvilinear response to VPD where V is highest at intermediate levels of VPD. Nevertheless, our results demonstrate that while environmental variables play a key role in transpiration dynamics, species differences and seasonality are potentially more important.

Such a conclusion is, of course, dependent on the range of variation in environmental variables, and the observed range of VPD values in our study was very small. Typical VPD in dry environments may be larger than 4 kPa and is rising globally in most ecosystems around the world (Grossiord et al. 2020). In our study though, high VPD is rarely as large as 2 kPa – and trees may have not experienced high VPD associated with dramatic declines in transpiration. Soil moisture values may have been much more variable, but despite low soil moisture values measured in this study, a test of tree water stress conducted on all tree species at the height of summer drought in 2023 using a Scholander pressure chamber (Kaufman 1968) indicated low water stress in all trees (Appendix A: Water Stress Measurement). Accordingly, it is likely that trees were able to access deeper sources of water during even the most stressful times of year in our study.

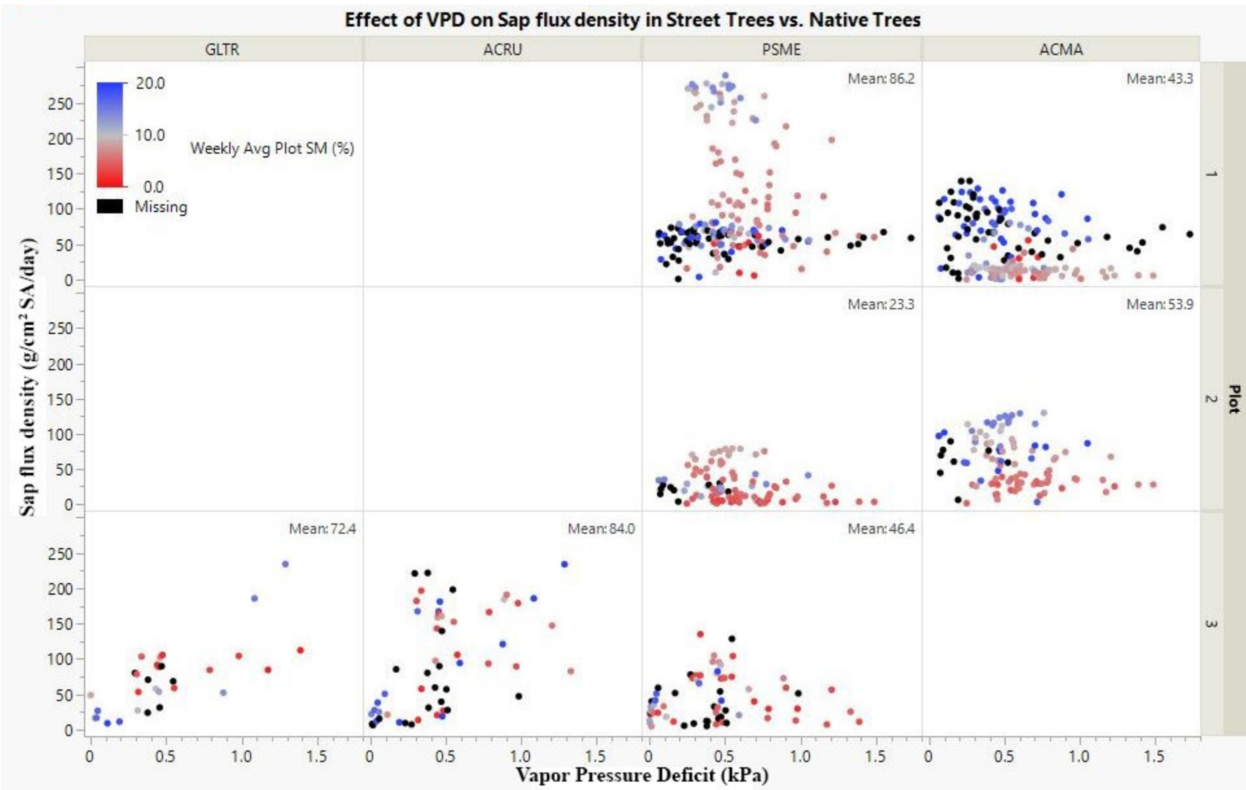

Figure 18. Depiction of daily sap flux density (V) by atmospheric vapor pressure deficit (VPD). Values are color-coded by soil moisture, where red values indicate low soil moisture, blue indicates high soil moisture, and black indicates days when soil moisture data. Plots 1 and 2 represent fixed station measurements in intact forest. Plot 3 represents street trees sampled in this study.

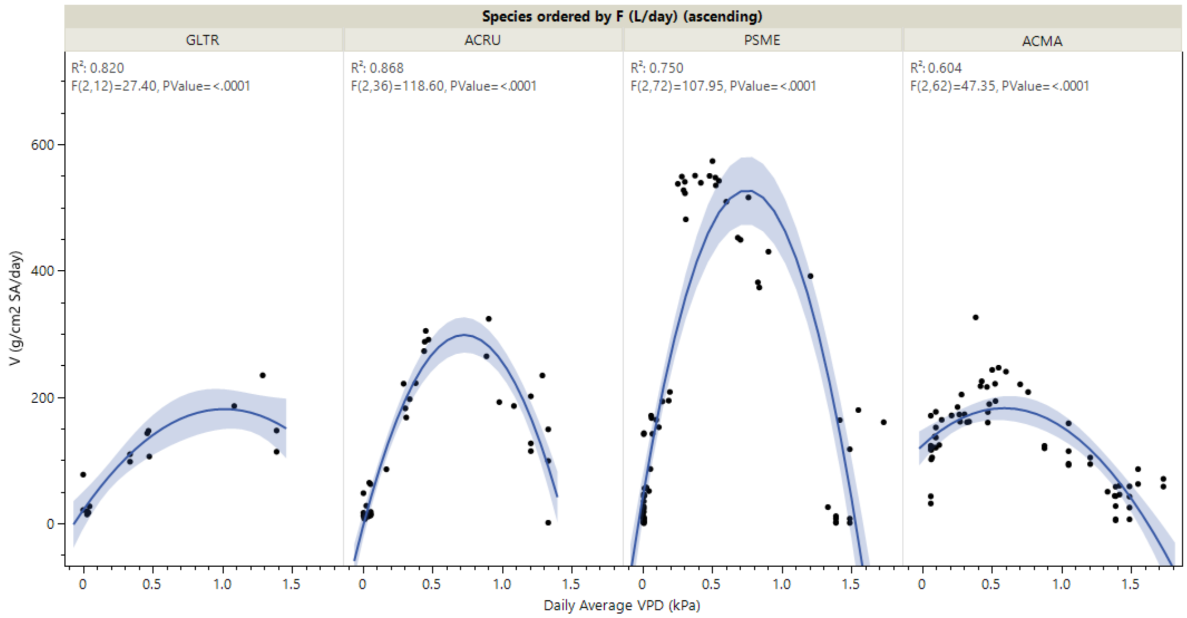

Figure 19. Depiction of daily sap flux density (V) by daily average atmospheric vapor pressure deficit (VPD) using boundary line analysis (excluding 1814 values shown in Figure 17 that were below the top of the response curves). All study sites are combined for this analysis. Regression analysis results are shown in each panel.

As in Phase I, our results showed that bigleaf maples (ACMA), on average, transpired at a higher rate (Figure 20-21). Douglas-fir (PSME) generally transpired more water during the shoulder seasons, and much less during mid-summer dry periods – a potential adaptation to summer drought. Coniferous trees can harness the high VPD days in the early spring and late fall to continue transpiring at high sap flux density rates (Figure 20-21). In the fall season, this was observed as rainfall that replenished soil water content and reduced VPD, which may have previously limited coniferous transpiration. During this time, deciduous transpiration dropped rapidly at the onset of senescence before complete defoliation (leaf-off). In late winter and early spring, an extended shoulder season advantage for coniferous trees was noted in March during high VPD days preceding the leaf-on transition period for deciduous trees in April. These patterns were also observed for street trees (Figures 20- 22).

Estimates scaled to whole trees show realistic estimates of daily transpiration that scale strongly with tree size, but especially for native trees which were much larger (Figure 23).

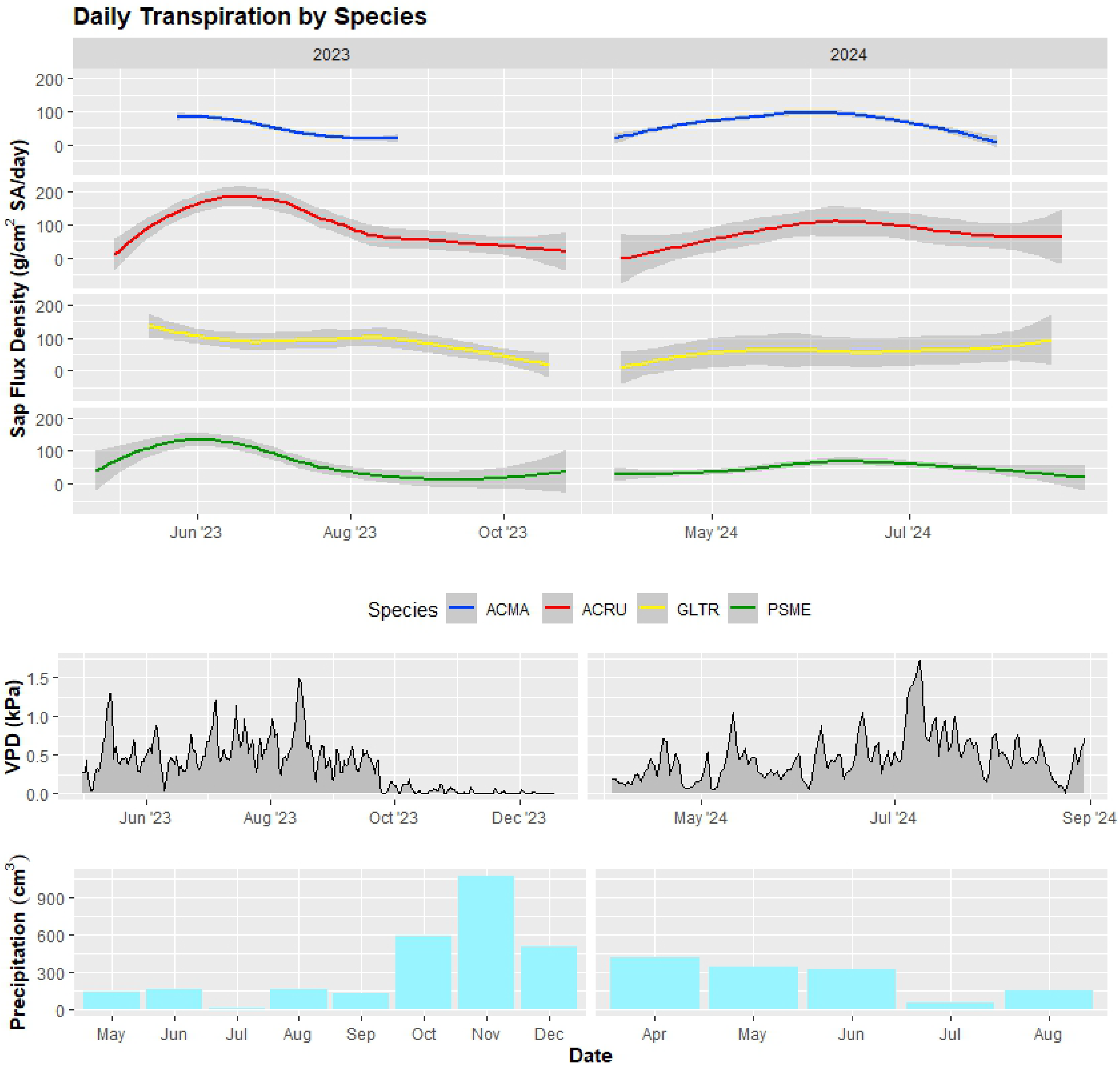

Figure 20. Annual patterns in average daily sap flux density for all species, vapor pressure deficit (VPD; middle panel), and precipitation (bottom panel) in the Phase II study.

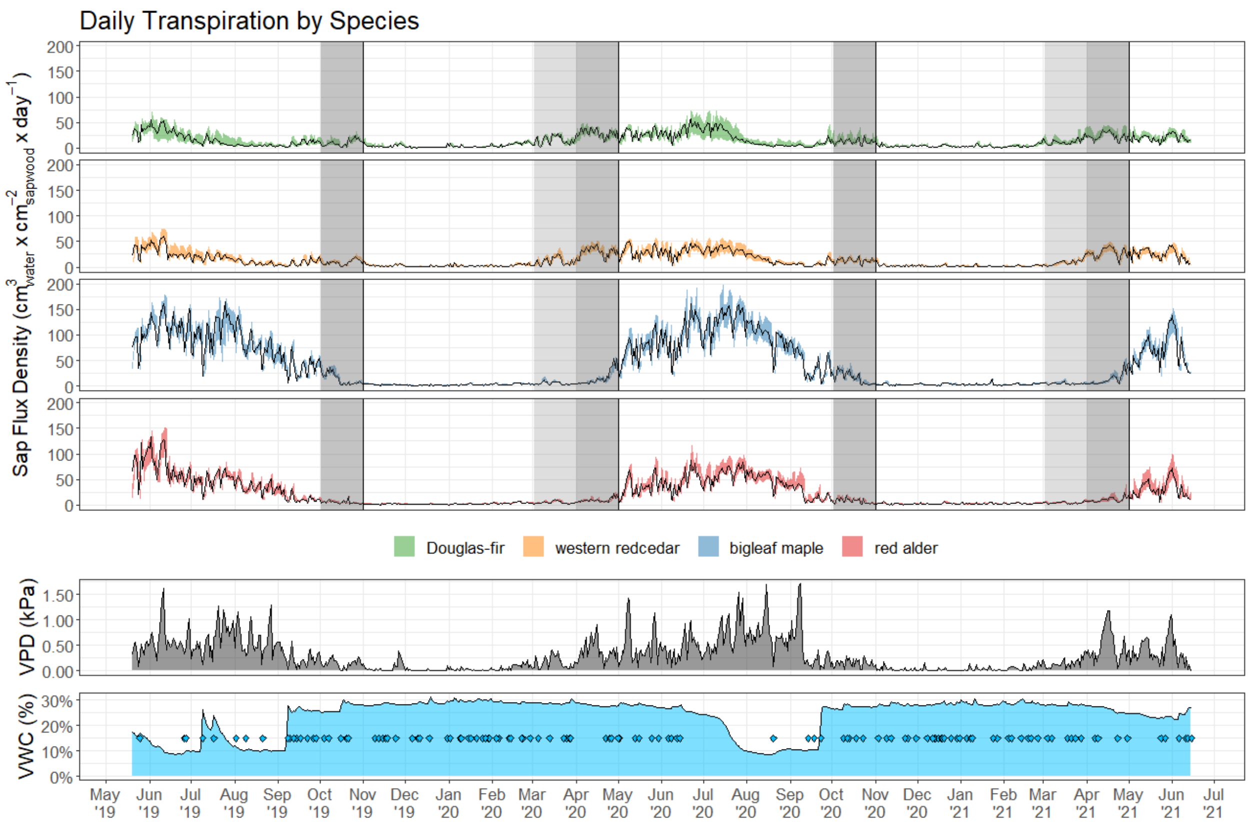

Figure 21. Phase I results presented here for comparison with Figure 20. Temporal distributions of median daily sap flux densities by tree species with inter-quartile range (IQR) shaded. Coniferous species exhibit high sap flux densities during the shoulder season when the deciduous trees are ramping up or ramping down (dark gray). March is shaded as an extended shoulder month (light gray). Leaf-on and leaf-off are separated by a black vertical line. Plots below show average daily vapor pressure deficit (VPD) and weather station soil volumetric water content (VWC; blue diamonds indicate qualify storm precipitation).

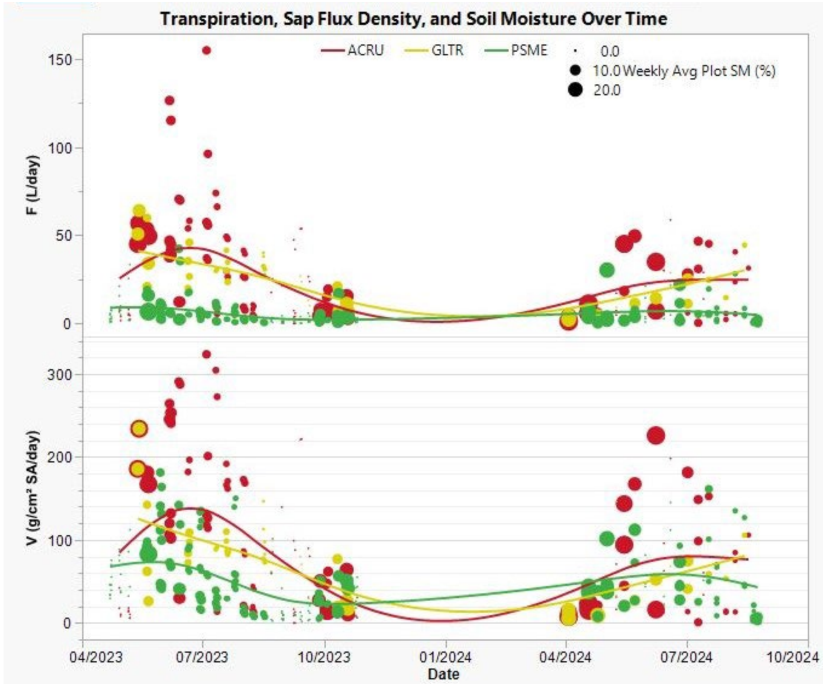

Figure 22. Temporal distributions of median daily sap flux densities by street-tree species. Coniferous species exhibited high sap flux densities (V) during the shoulder season when the deciduous trees ramped up or down. Point size scales with soil moisture availability where larger points indicate greater soil moisture. Whole tree transpiration scales with tree size, and since PSME were generally smaller trees, they had lower transpiration (F) values. Transpiration was not measured during the leaf-off winter and early spring seasons of 2024.

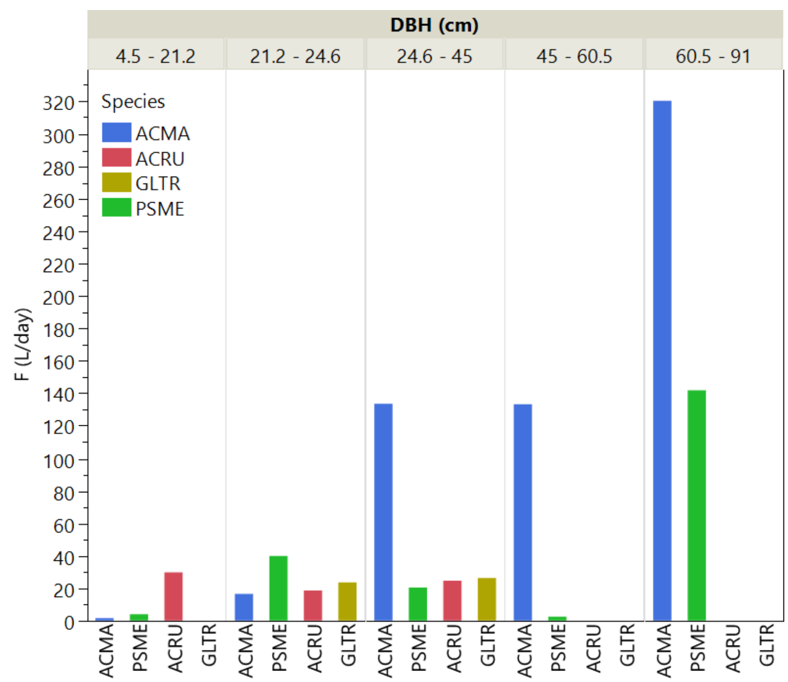

Figure 23. Total tree transpiration (average) for all tree species (x-axis) measured in the study across a range of tree sizes.

Individual Tree Water Budgets

Individual tree transpiration and interception rates depend on tree size and canopy area. Because sapwood area scales with tree size, larger trees have greater influences on transpiration (F; Figure 16). Nevertheless, the relationship can be variable even in young trees is sap flux velocity (V) rates decline with increasing tree size. Accordingly, calculating whole tree F is important for understanding tree water budgets. Similarly, tree canopy size, and thus interception (due to greater canopy area), also increase with tree size. Additionally, the tree leaf area index (leaf area per unit ground surface) increases with tree age and height, where taller trees have more opportunities for a layered leaf structure that maximizes area per ground surface. Thus, larger trees inherently transpire more water where tree water-use scales directly with tree bole size (DBH; Figure 16) and similarly interception scales with tree size, canopy size, and leaf area.

Predicting the impact of trees on local water budgets and stormwater also depends on tree species and the timing of precipitation, maximum interception, and transpiration. Species differences in interception can significantly impact annual estimates (see Phase I results), especially when spatial patterns are considered (Fischer et al., 2022). Additionally, the timing of transpiration and interception may not correspond with maximum stormwater runoff, and tree water budgets should be considered in the context of when storm surges occur. Table 4 shows results for all trees including forest (Plots 1 and 2) and street (Plot 3) trees. Across all trees, annualized values demonstrated that tree transpiration and interception mitigated 42-66% of precipitation inputs, and values were higher for street trees (61-66%) compared to forest trees (42-53%), likely due to both fuller canopies (high LAI) and limited reductions in transpiration at high VPD.

Table 4. Median values representing contributions to stormwater mitigation by each species are shown for each year in the study period as a percent of total precipitation and amount in centimeters.

Individual Tree Contributions to Stormwater Mitigation						
	2023		**2024**		**Annualized Values**	
	Median Values by Species (Transpiration + Interception)					
Tree Species	%	cm	%	cm	%	cm
Bigleaf maple	27.6%	34.4	126.5%	54.3	52.9%	88.7
Douglas-fir	30.6%	38.2	76.2%	32.7	42.3%	70.9
Honey locust (street tree)	57.2%	71.4	73.1%	31.3	61.3%	102.7
Red maple hybrid (street tree)	63.3%	79.0	72.6%	31.1	65.7%	110.1

Conclusions & Key Findings

The study examined: 1) relationships between tree diameter and sap flux velocity in tree stems (V); 2) agreement in patterns of V between traditional fixed-station measurements and a newer mobile sap flux technology design; and 3) patterns in both V and whole tree transpiration for street trees in a parking lot setting as a model for urban street tree transpiration.

PIC:

Tree size effects.

Our results show that tree size does have a predictable relationship with transpiration when using all trees in the study across the entire study time. Nevertheless, when considering only coincident days (when measurements were taken coincidentally for all tree sizes), we found a lack of significant relationship between tree size and V. Without a significant tree size effect, scaling of our results from Phase I could be justified based on the use of average V values by species. We suggest this approach is reasonable for future studies that cannot account for tree size variation. Estimates of V from studies such as ours likely can provide robust estimates of sap flow movement for similar trees across the region.

PIIE:

Validation of the Mobile Probe Method.

Our results showed agreement between methods and mobile probe approaches, which provided robust estimates of tree sap flux over two years. Accordingly, we recommend that this method can produce reliable estimates in other locations and should be used better to gain information about sap flux patterns in street trees.

Interception and Street Tree Water Use: Interception was quantified for both conifer and deciduous species, as well as forest and street trees. Our data validate that interception can be different among species and contribute to a high amount of variation in the annual water budget of a given tree. Interestingly, our Phase II results highlight higher total mitigation (transpiration and interception) values for street trees. Both deciduous street trees considered in this study showed combined transpiration and interception impacts greater than 50% of precipitation during the study period (50-73%). Similarly, street tree Douglas-fir had values between 30 and 76% of precipitation. Transpiration was highly dependent on season, but estimates were similar to estimates based on forest tree measurements, suggesting that soil water did not generally limit transpiration in 2023 and 2024, except in the dryest months of the year.

Recommendations: Our results generally confirm findings in Phase 1, suggesting sap flux density (V) values are scalable across tree sizes from small street trees to large remnant legacy trees among deciduous and conifer species examined. Street Tree V values were similar to forested tree values. However, the whole tree sapwood area scales with tree size, and thus, greater tree sizes will have greater influences on transpiration (F; Figure 15), interception (due to greater canopy area), and overall hydrologic budgets. Our results validated results from Phase I and suggest increasing sampling numbers to include additional street trees will provide valuable information to city planners, urban foresters, and stormwater managers who might be interested in considering other tree species in urban communities. Our limited sampling of street trees suggests that these trees can have large effects on mitigating precipitation inputs to impervious surfaces. There is also tremendous potential offered by the mobile sensors developed through this study to engage communities across Washington in the hydrologic valuation of urban trees, whilst also collecting information on co-benefits these trees offer urban communities. The mobile sensors were shown to be robust, discrete, and capable of providing accurate information.

References

Brady, N.C., Weil, R.R. and Weil, R.R., 2008. The nature and properties of soils. Prentice Hall, NJ.

Benedict, S.R., 1909. A reagent for the detection of reducing sugars. *Journal of Biological Chemistry*, 5(5), pp.485-487.

Fischer, D.G., Kolb, T.E. and DeWald, L.E., 2002. Changes in whole-tree water relations during ontogeny of Pinus flexilis and Pinus ponderosa in a high-elevation meadow. *Tree Physiology*, 22(10), pp.675-685.

Fischer, D.G., Vieira, S.T. and Jayakaran, A.D., 2023. Distinct rainfall interception profiles among four common Pacific Northwest tree species. *Forests*, 14(1), p.144.

Granier, A. 1985. A new method of sap flow measurement in tree stems. *Annales des Sciences Forestières*. 42(2), pp. 193-200

Granier, A. and Loustau, D., 1994. Measuring and modelling the transpiration of a maritime pine canopy from sap-flow data. *Agricultural and Forest Meteorology*, 71(1-2), pp.61-81

Grossiord, C., Buckley, T.N., Cernusak, L.A., Novick, K.A., Poulter, B., Siegwolf, R.T., Sperry, J.S. and McDowell, N.G., 2020. Plant responses to rising vapor pressure deficit*. New phytologist*, 226(6), pp.1550-1566.

Jayakaran, A., Leonard, B., Fischer, D., Duberstein, J., Barnes, A., 2022. Measuring Individual Tree Water-use in Mature Native Species in the Pacific Northwest to Determine their Benefits for Stormwater Management: Final Report. https://ecology.wa.gov/regulations-permits/reporting-requirements/stormwater-monitoring/stormwater-action-monitoring/sam-effectiveness-studies.

Kaufman, M.R. 1968. Evaluation of the Pressure Chamber Technique for Estimating Plant Water Potential in Forest Tree Species. *Forest Science*. 14, pp. 369-374.

Kutscha, N.P. and Sachs, I.B., 1962. Color tests for differentiating heartwood and sapwood in certain softwood tree species (Report 2246). United States Department of Agriculture and Forest Service, Madison, WI, USA.

Oishi, A. Christopher; Hawthorne, David A.; Oren, Ram. 2016. Baseliner: an open source, interactive tool for processing sap flux data from thermal dissipation probes. Software X 5(139-143) p. 10.1016/j.softx.2016.07.003

Scholander P.F., Bradstreet, E.D., Hemmingsen, E.A., and Hammel, H.T. 1965. Sap pressure in vascular plants: Negative hydrostatic pressure can be measured in plants. *Science* 148, pp. 339–346

Steppe, K., De Pauw, D.J., Doody, T.M. and Teskey, R.O., 2010. A comparison of sap flux density using thermal dissipation, heat pulse velocity and heat field deformation methods. *Agricultural and Forest Meteorology*, 150(7-8), pp.1046-1056.

Appendix A: Methods of Environmental Data Collection in this Study

Soil Moisture

Among all groups of sensors deployed for Phase 1, soil moisture probes proved the least reliable. In many cases, sensors failed after water penetrated the mote's weatherproofing and corroded the data logger's circuitry. In other cases, data was determined to be unreliable when plotted and thereby abandoned. However, of the five probes initially deployed per plot, at least two per plot could provide a continuous data stream during the study duration. Measurements from capacitance probes were supplemented by time-domain reflectometry (TDR) probes deployed throughout the study to provide quality assurance.

For Phase 2 of this study, TDR measured soil moisture directly using a Hydrosense II Soil Moisture Measurement tool (Campbell Scientific, Inc.). A technician collected four measurements at each tree 1 m from the tree base in each cardinal direction weekly. An average was then calculated for each tree. In the parking lot, weekly soil moisture was only captured for each tree being measured for sap flux. At the forest site, every tree was measured each week. When volumetric water content was expected to be high (> 22%) or low (< 4%), soil moisture was not sampled (early spring, mid-summer, late fall). Generally, a reading of greater than 40% soil moisture was associated with standing water. Observations of standing water suggest soil saturation, at which all pores are filled with water, and occurs at a range of volumetric water content values from 30 to 60% for sandy to clay soils (Brady et al. 2008). Soil moisture was routinely higher for trees northwest of the Evergreen Forest site. These trees were unintentionally distributed across a shallow elevation gradient extending 81 m northwest-to-southeast.

Soil moisture measurements aimed to assess general soil conditions that may impact tree water availability for transpiration. Patterns of soil wetting associated with throughfall from rain events were also interesting but were not intended to be thoroughly evaluated. No effort was taken to quantify further soil properties such as soil type, water potential, hydraulic conductivity, nutrient levels, or organic carbon content. Therefore, it is essential to note that soil moisture results should be considered semi-quantitative at best without additional context.

While soil saturation is one crucial consequence of winter flooding, tree health and water use are not likely to be adversely impacted by a short-term excess of soil water. This is especially true of the native trees studied, which may be adapted to such environments and have relatively low metabolic requirements during winter. Two exceptions would be root rot from sustained inundation and tree fall from bank erosion, neither of which was observed for the study trees. More importantly, low soil moisture during prolonged summer droughts has the potential to limit water use via transpiration.

While it was not a study objective to properly determine the field capacity and permanent wilting points of the plot soils, it was expected that volumetric water content values below 10 to 15% increasingly resulted in drought stress. The permanent wilting point, at which trees can no longer absorb water through their roots, generally ranges from 4 to 22% volumetric water content in sandy to clay soils, respectively (Brady et al. 2008). The soil at both sites is Pleistocene continental glacial till with a mix of sand, silt, and clay, but with higher clay content and greater compaction in the Evergreen Parking Lot (https://websoilsurvey.nrcs.usda.gov/app/, last accessed 10/31/2024). Therefore, it is likely that the volumetric water content associated with permanent wilting point is slightly higher at the Evergreen Parking lot site, but these locations do not represent extremes for soil composition.

Water Stress Measurement

In the peak of drought conditions in 2023, we performed a 1-day test of tree water status by examining midday water stress in each tree species. We use a Scholander pressure chamber (Scholander et al. 1965, Kaufman 1968) to examine water pressure in 0.5-1.5 cm diameter excised stems from each tree species between 12 PM and 4 PM on August 16th and 17th in 2023. 3-4 stems were examined for each species and only values within 0.5 MPa were accepted as reliable. Data demonstrated that ACMA trees in the study had the least water stress in this period, while GLTR trees saw the highest water stress (indicated by low negative values, Figure A1)

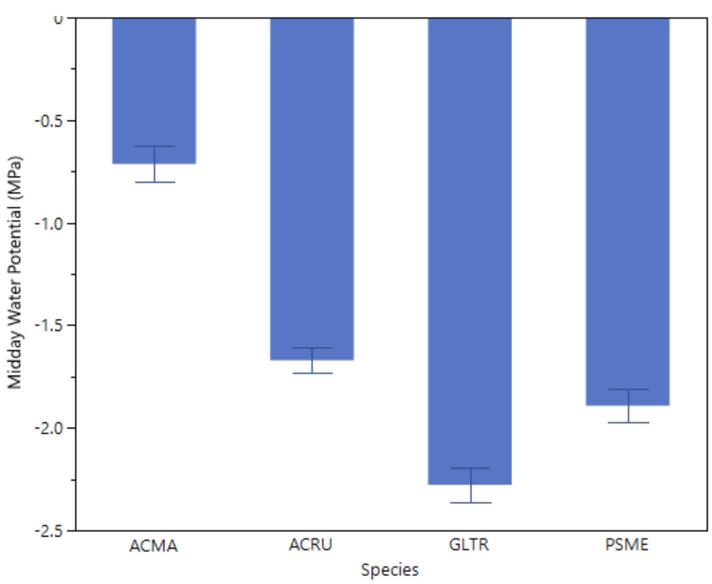

Figure A1. Water stress in species studies in Phase II of the project. Negative values below 2 are generally associated with water stress, but drought adapted species such as GLTR are known to tolerate negative values far below -3 MPa.

Vapor Pressure Density

Vapor Pressure Density (VPD) is calculated from measurements of air temperature and relative humidity using a standard equation based on Tetens formula where the saturated vapor pressure is calculated as

$$e_s(millibars) = e^{\left(\frac{(17.269*T)}{(237.3+T)}\right)} \times 6.1078$$

where e_s is saturated vapor pressure in millibars, T is temperature in °C, and vapor pressure deficit is calculated as

$$VPD = e_s - \frac{Rh \times e_s}{100}$$

Where *Rh* is relative humidity.

Interception Estimates

Throughfall

Sixteen trees were instrumented for the measurement of interception using RXW Davis Rain Gauge Sensors (Onset, HOBO Data Loggers). Measurements used a simplified approach compared to Phase I, where individual precipitation gauges were placed directly under tree canopies (see methods above).

We also used simplified methods for tree canopy size determination to be consistent with what managers and technicians are more likely to measure in the field (namely, canopy widths to dripline).

In practice, a tree's canopy is rarely uniform in shape and often overlaps with the canopies of nearby trees. This is especially true of the more natural areas where residual stands of mature native trees are typically found. This study made several practical concessions, as detailed in the methods below—the Final Report for Phase I should be considered for a more detailed consideration of the throughfall problem. Fischer et al. (2023) also provide a detailed species-by-species analysis of interception patterns at our site.

Transpiration By Sap Flux

Installation

The following text is modified from Phase I of our initial work. It represents the general methods for Granier sap flux measurement (Granier et al. 1994) in greater detail than provided in the methods above:

Sap flux was measured using the thermal dissipation probe (TPD) method, as first described by Granier (Granier 1985). TDP systems were manufactured by Dynamax Inc. (FLGS-TDP XM1000 Sap Velocity Logger System). They consisted of a data logger (Campbell Scientific CR-1000X), an adjustable voltage regulator (AVRD), and several types of probes capable of measuring sap flux at a variety of depths (15, 25, 50, 70, and 90 mm).

Two cylindrical probes, 1.75 mm in diameter, were inserted radially into parallel holes drilled 40 mm apart vertically in the tree's xylem. Four lengths of probes were used in the study, 30, 50, 80, and 100 mm, providing measurements at 15, 25, 15 and 70, and 15, 50, and 90 mm respectively. Out of 40 trees in this study, 10 were measured at more than one depth.

The upper probe was supplied with a constant voltage and was continuously heated, while the bottom probe, unaffected by the heat, provided reference measurements. The difference in temperature between the upper and lower probe (ΔT or dT) was sampled every minute and recorded as 15-minute averages.

Data Gaps

During the two years of data collection, several logistical issues prevented uninterrupted continuous TDP data collection. These were to be expected, and some redundancy was incorporated into the study plan to address this. Nevertheless, data was filtered to avoid skewed data associated with power interruptions, heat spikes, probe malfunctions, and incomplete measurement days.

Data Processing

As the tree transpires, the rate of water movement through the principal stem increases, and the heated top probe is cooled. As a result, the difference in temperature between the two probes decreases. To calculate sap flux via the Granier method, it is typically assumed that there is a point of zero sap flux every 24 hours, which is observed as the local maxima of dT. Each subsequent observation for a 24-hour cycle is then normalized by dTMax, and the dimensionless "flow index," K, is computed. While dTMax is often assumed to be constant every 24 hours, this assumption results in a sudden change in sap flux as dTMax shifts. To address this issue, dTMax was interpolated with a continuous linear approximation based on the methodology provided by default in the program Baseliner (Oishi 2016).

$$K = \frac{\Delta T_m - \Delta T}{\Delta T}$$

To calculate sap flux, the Granier equation includes two empirical coefficients where $\alpha = 0.0119$, $\beta = 1.231$, and V is sap flux in cm^3 of water per cm^2 of sapwood per second.

$$V = \alpha \times K^{\beta}$$

Uncertainty

The Granier method makes two critical assumptions:

a) Nighttime sap flux is negligible, meaning that pre-dawn dTMax can be used to calibrate zero sap flux.

This assumption is a critical underpinning of the Granier method. Several studies have suggested this to be one crucial factor for TDPs under-estimating transpiration compared to other methods (Steppe et al. 2010).

b) Sap flux moves in one direction, up the tree, and the tree does not move water from the crown to the roots.

The two-probe TDP setup cannot accurately measure "reverse sap flux"; the sap flux rate is always greater than or equal to 0. Any reverse sap flux in our data set would be indistinguishable from dTMax estimates. This variation source should be considered when using data from the present study.

Sapwood Area

For many conifers, including Douglas-fir (*Pseudotsuga menziesii*), the boundary between wet sapwood and dry heartwood is often determined visually. The sapwood boundary, which may be observed and measured using a sample obtained from an increment borer, occurs at the transition between light and dark wood (Kutscha and Sachs 1962). Lighter color sapwood indicates elevated water content and intact pores within xylem, while darker heartwood is rich with tannins and resins, making it far less hydraulically active.

In Douglas-fir, when the sapwood transition was not obvious, the core was exposed to a pH indicator solution (bromocresol green), sensitive to the hydrogen activity of phenolic compounds in the heartwood. The exact pH indicator solution did not highlight sapwood in the deciduous tree species. Benedict's solution (Benedict 1909) was found to indicate sapwood in Bigleaf Maple effectively.

In the photograph below, a Douglas-fir core is being measured for the sapwood area. The extent of the blue/green stain is indicative of sapwood. More porous earlywood rings absorbed more dye, creating a striped appearance. When the sapwood boundary was located at the edge of an earlywood to latewood transition, the latewood midpoint was used. This difference was typically less than 2 mm.

Figure A2. Bromocresol green stained sapwood in several Douglas-fir core samples.

For the deciduous species in this study, bigleaf maple (*Acer macrophyllum*), the transition between sapwood and heartwood is less visually evident due to the complexity of their vascular tissue anatomy. To properly assess sapwood depth in deciduous species, various techniques were used during Phase 1.

Sapwood depth in deciduous trees for Phase 2 was measured visually to the nearest millimeter and verified by a second observer. Benedict's solution was used when the sapwood boundary was difficult to distinguish from late- and earlywood boundaries.

Censoring and Data QC

This section is modified from the Phase 1 report but includes updated information about our approach to data censoring and quality control.

While TDPs are considered a robust and reliable method for measuring sap flux, it is essential to qualify data that may be compromised by electrical issues associated with probe deployment. These data should be censored and removed from the dataset because they do not reflect actual sap flux. Considering the frequency of measurements, number of probes and wires, need for constant power, and harsh environmental conditions, it was expected that some significant portion of the dataset would need to be censored.

Censoring TDP data was mostly a manual process. During data collection, most data issues were observed through time series raw data plots using Campbell PC400. Values for dT are typically within the range of 2 and 30° C, and TDP data outside this range were flagged for further investigation. Data were also flagged if the slope between measurements exceeded one, which was often observed for wiring issues. All flagged observations were then plotted to manually determine the potential cause and extent of the data issue.

The most common cause of erroneous TDP data was corrosion caused by water penetrating the sealed connections between the data logger and probe. If this issue was suspected during data collection, the probe and wiring were inspected with a multimeter to confirm the continuity of power. After determining the source of the error, the appropriate piece of equipment was replaced, usually within 48 hours. Equipment failure resulted in a data gap for the associated tree until the issue was resolved.

Several steps were taken to mitigate this reoccurring issue in Phase 1, including weatherproofing and lifting cable junctions off the ground. However, this pervasive issue continued throughout the study, including Phase 2. Similarly, intermittent shorts were sometimes experienced when cables kinked or overlapped. Most connectivity issues manifested when noisy signals were plotted outside the typical dT range (2-20° C).

In addition to “noise,” we also observed “spikes,” which were most likely caused by power surges. These were usually easy to identify from time series plots and often resulted in only a few 15-minute measurements being censored. The resultant data gap was subsequently interpolated using the program Baseliner (Oishi 2016).

Lastly, each plot had at least one power failure during the study. This resulted from a tripped GFCI plug that needed to be reset, a power outage from a winter storm, or a malfunctioning trickle charger. Since each TDP station was powered by a 12 V marine-grade deep cycle lead-acid battery that was being charged via a 120 V AC outlet, station power remained on for up to 48 hours after power failure. The data produced surrounding a power failure often consisted of many “spikes” that had to be censored. Considering the frequency of result data gaps, it was not appropriate to interpolate data, and days associated with power failures were consequently censored.

Instructions (SOP) for construction of mobile sap flux units.

SOP for building mobile tree units (CT notes)

1. Build RTC/data logging shield *weeks* before assembling the rest of the MTU. (4:57)
    a. The Kit comes with pins. Use the set with a divider piece.
    b. Use breadboard, solder pins to RTC (small end on top, long end on bottom)
    c. Remove 2 diodes
    d. Insert the battery (c1220, 3v), make a note of battery voltage
    e. Insert SD card if desired—must be a fat 32 formatted SD card, else the HD or SD card WON'T work)
    f. Insert into test MTU, connect to a computer.
        i. Run clock program
        ii. Run MTU program
    g. Periodically (about 2 weeks or more), recheck clock with MTU code/computer and battery voltage.
    h. If it has not drained the battery, it is ready to use in MTU
2. PCB board (0:00)
    a. Pull the pins from the Arduino kit
    b. Easiest to place them in the Arduino board and break them off to the right size
    c. Set them up on Arduino, place PCB board on top and solder them to PCB board
3. Blue Screw terminals (3:11)
    a. 11 terminals (3 x 3 terminals plus 1 x 2 terminal pieces)
    b. Slide them together
    c. Solder them on to the PCB board, with terminals facing out (for sensors wires to be put in)
4. RTC/data logging shield (4:57)
    a. If the RTC has been tested and ready to go, solder it on top of the PCB board
    b. Electrical tap does a good job holding this piece in place and tight since soldering upside down.
    c. Trim pins
5. Voltage regulator (7:29)
    a. Use a piece of foam with slot for voltage regulator to be stabilized. Propped up other side opposite blue screw terminals with other blue terminal pieces.
    b. Solder in place, black box faces the edge of board
    c. Trim long pieces off
6. Capacitors (x2) (8:20)
    a. Long end is positive, this is important for placement—look at PCB board
    b. Flatten edges then pull through and fold down
    c. Solder on. Trim long pieces off.
7. Resistors (10:50)
    a. 220 Ohm. Possible combinations:
        i. Red, red, black, black, gold

ii. Red, red, brown, gold
iii. Solder in (direction doesn't matter)
iv. Cut long pieces off

8. Gain amplifier (11:53)
   a. Comes with pins in a bag. The correct placement has the black box "on top."
   b. Use bread board to place pins with amplifier on top. Solder
   c. Then set the amplifier on the bottom of the PCB (make sure labels on amplifier match locations on PCB)
   d. Tape amplifier to board for soldering (cut piece of tape in half lengthwise)
   e. Trim pins
9. Buck Converter (12:53)
   a. Need to use long pins, cut them off one at a time using blue snips
   b. Set pins on bread board
      i. C & G @ 65
      ii. C & G @ 39
      iii. Place buck converter on top of pins, solder them
   c. Final assembly to PCB board—match up with the "in" and "out" on the board
      i. Use piece of wood spacer between buck converter and PCB
         1. Make sure converter is not touching anything, especially RTC
      ii. Flip upside down and rest on foam piece—double check that 4 pins are even for converter.
      iii. Solder converter to PCB
      iv. Trim pins if needed
10. Arduino
   a. Place black electrical tape on top of port for connecting to computer
   b. May need to trim solder under blue screw terminals for PCB
11. On off on Switch (14:17)
   a. Build with black on the right, charge on the bottom and datalogger bare on top
   b. Use helping hands plus prop on needle nose pliers
   c. Use red handle crimper—one set of male ends, one set of female ends (red size)
12. Box prep (21:11)
   a. Cable gland hole—drill with black bit about ½ way
   b. On off on hole—use 15/64th bit
13. TDP "pigtail to datalogger (24:11)
   a. Connections
      - v- >> Black
      - V+ >> Red
      - Bare >> Bare
      - + >> white
      - - >> green

Arduino codes (30:37) tree pro version 3.0

Raw values to voltage (34:07)